

Supplements to Examining NHD vs QHD in the GCM THOR with non-grey radiative transfer for the hot Jupiter regime

Pascal A. Noti,^{1,2}★  Elspeth K. H. Lee,¹  Russell Deitrick³  and Mark Hammond⁴ 

¹*Center for Space and Habitability, Universität Bern, Gesellschaftsstrasse 6, CH-3012 Bern, Switzerland*

²*Physikalisches Institut, Universität Bern, Sidlerstrasse 5, CH-3012 Bern, Switzerland*

³*School of Earth and Ocean Sciences, University of Victoria, Victoria, British Columbia, Canada*

⁴*Atmospheric, Oceanic and Planetary Physics, University of Oxford, Oxford, United Kingdom*

Accepted XXX. Received YYY; in original form ZZZ

1 GCM SIMULATIONS

1.1 Altering Rotation Rate at low gravity

1.2 Altering Gravity

1.3 Altering Irradiance Temperature at low gravity

1.4 Altering Rotation Rate at high gravity

1.5 Altering Irradiance Temperature at high gravity

This paper has been typeset from a T_EX/L^AT_EX file prepared by the author.

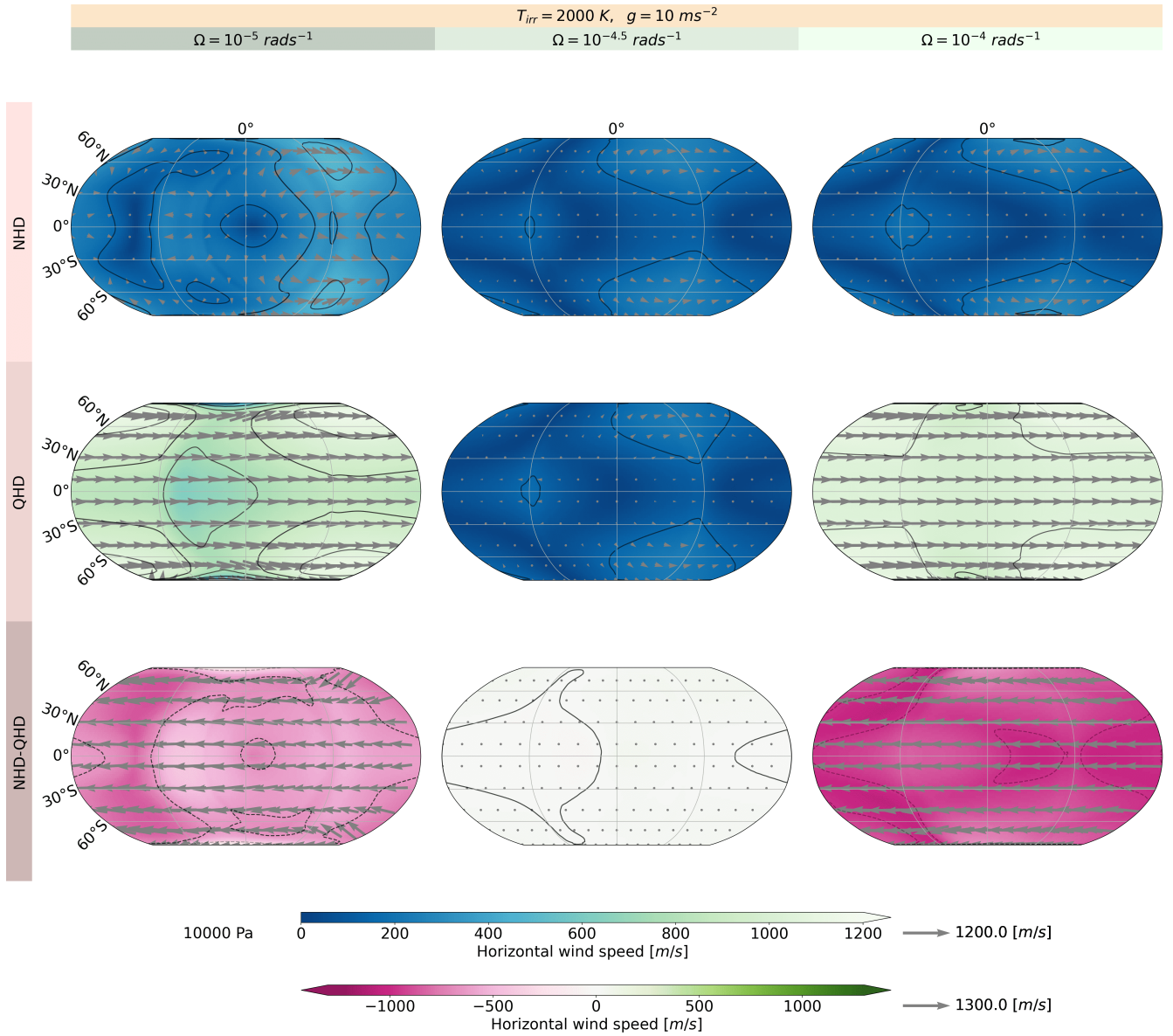


Figure 1. Horizontal wind speed at 10'000 Pa for the NHD and QHD equation sets with $g = 10 \text{ ms}^{-2}$, $T_{irr} = 2'000 \text{ K}$ and with altering Ω .

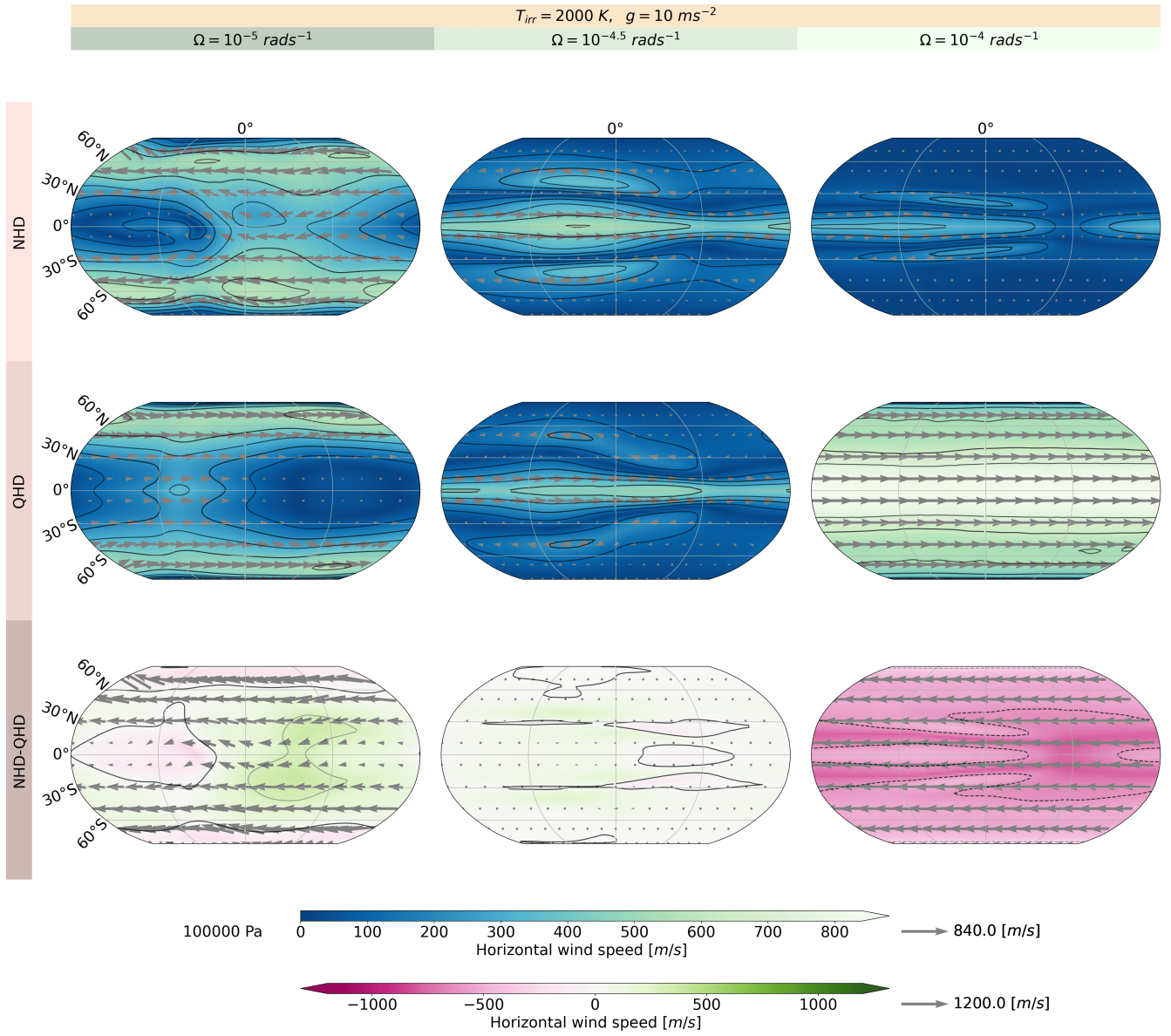


Figure 2. Horizontal wind speed at $100'000 \text{ Pa}$ for the NHD and QHD equation sets with $g = 10 \text{ ms}^{-2}$, $T_{irr} = 2'000 \text{ K}$ and with altering Ω .

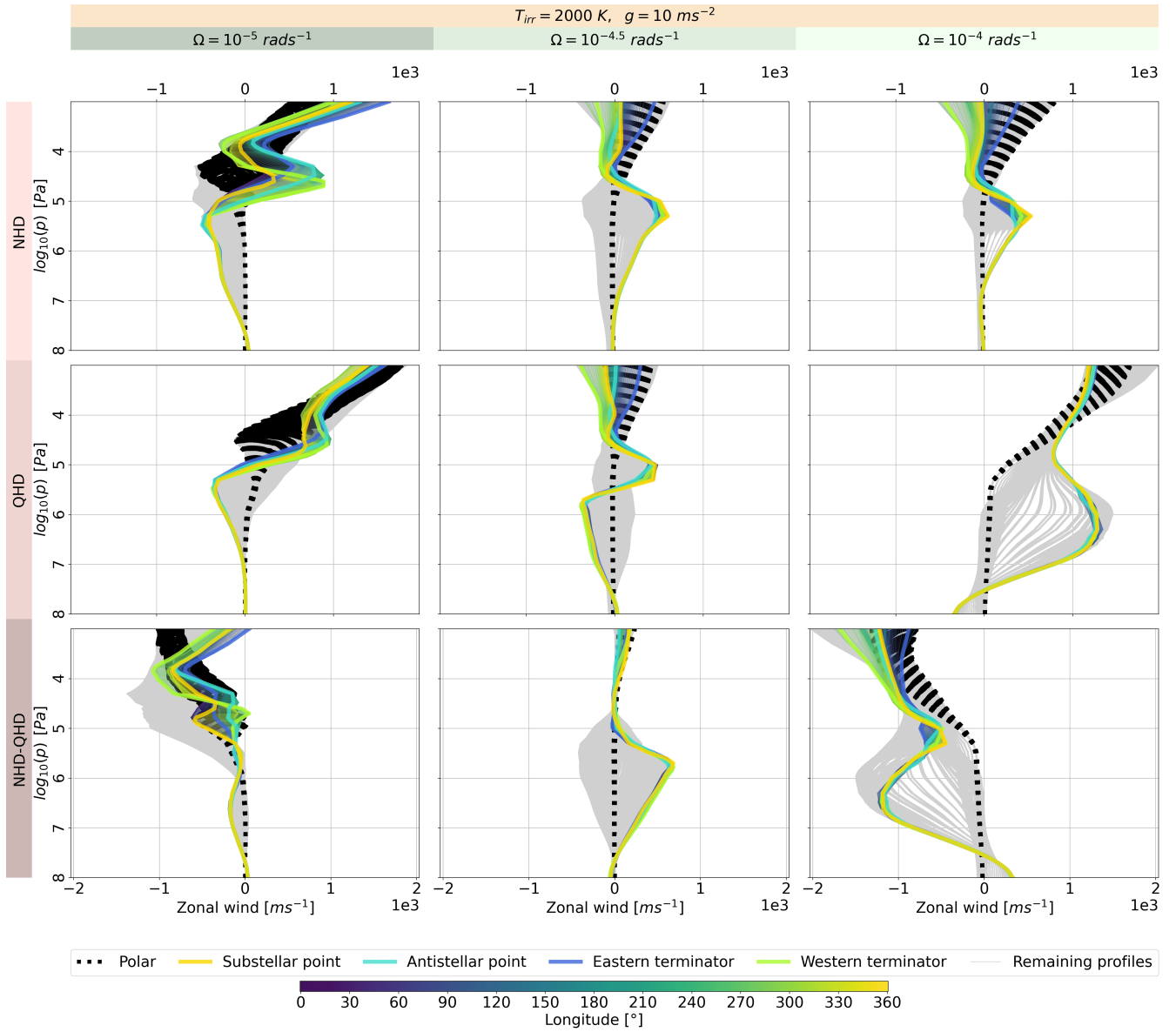


Figure 3. Zonal wind speed at each grid point for the NHD and QHD equation sets with $g = 10 \text{ ms}^{-2}$, $T_{irr} = 2'000 \text{ K}$ and with altering Ω . The coloured lines indicate momenta profiles along the equator and its coordinates by the colourbar. The dotted black thin line shows momenta profiles at the latitudes 87°N and 87°S . The bold coloured lines represent momenta profiles at the western, eastern terminators, sub- and antistellar point. The grey lines represents all the other momenta profiles.

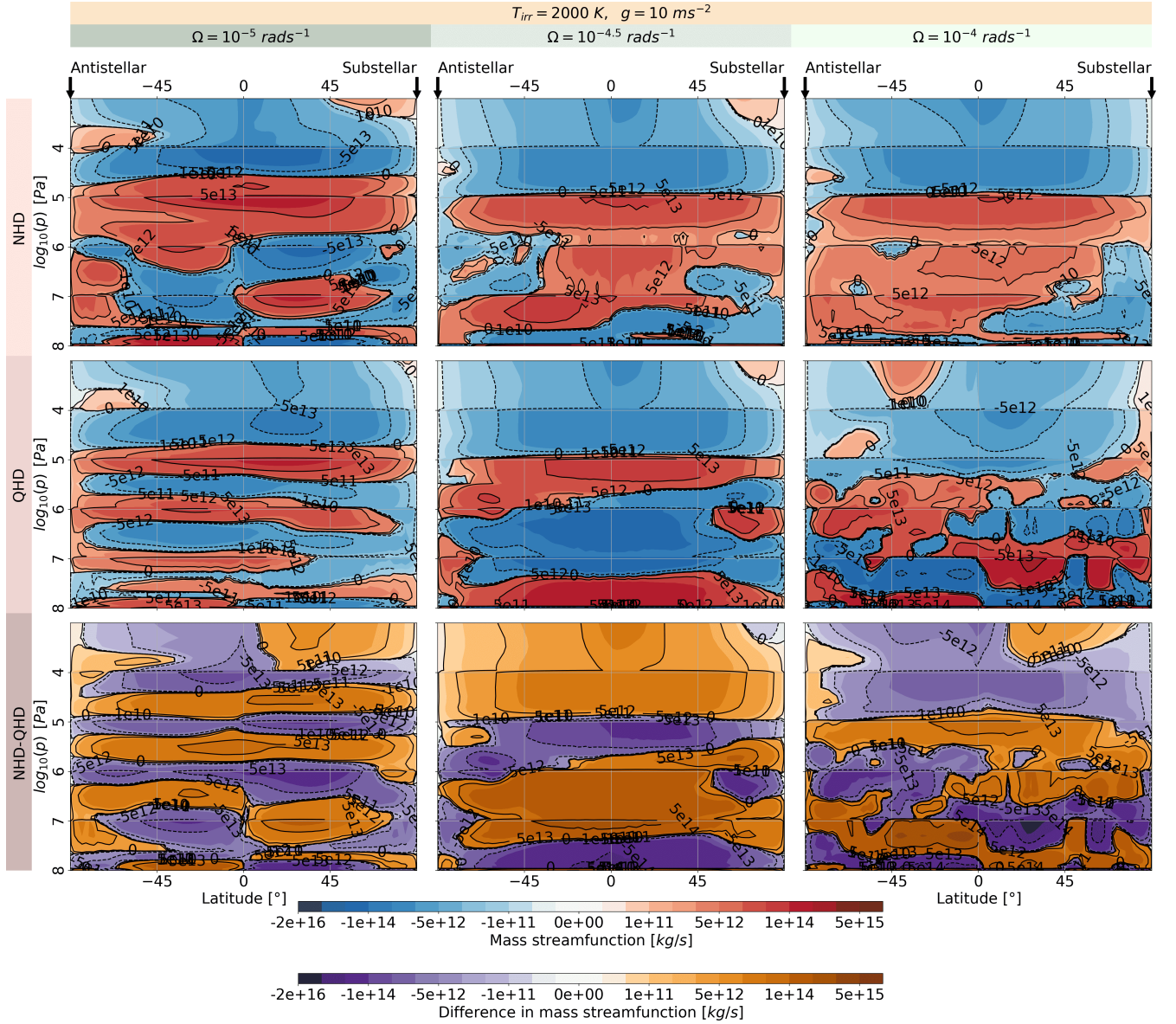


Figure 4. Overturning circulation depicted by the streamfunction Ψ' for the NHD and QHD equation sets with $g = 10 \text{ ms}^{-2}$, $T_{\text{irr}} = 2'000 \text{ K}$ and with altering Ω .

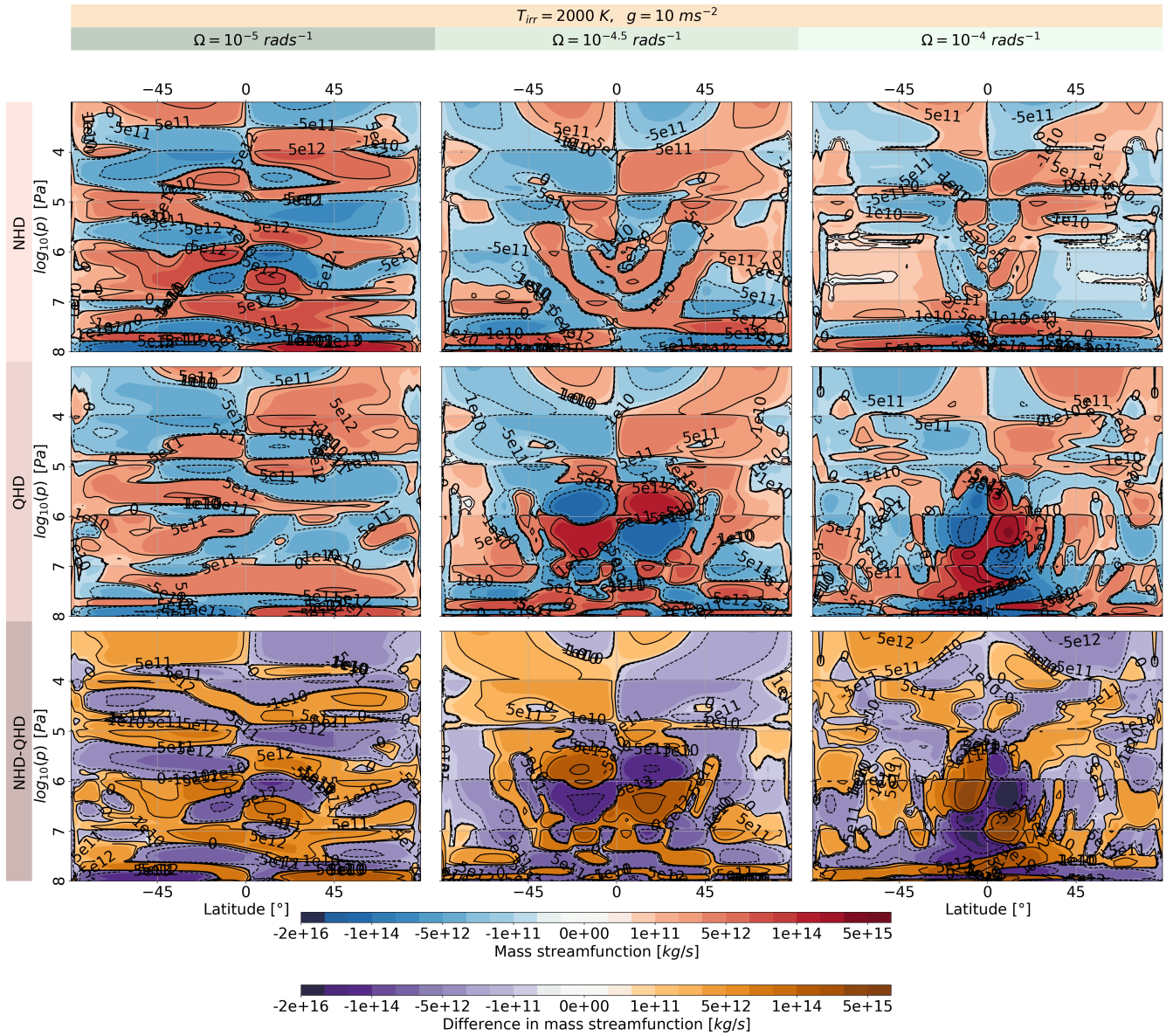


Figure 5. Overturning circulation depicted by the streamfunction Ψ for the NHD and QHD equation sets with $g = 10 \text{ ms}^{-2}$, $T_{irr} = 2'000 \text{ K}$ and with altering Ω .

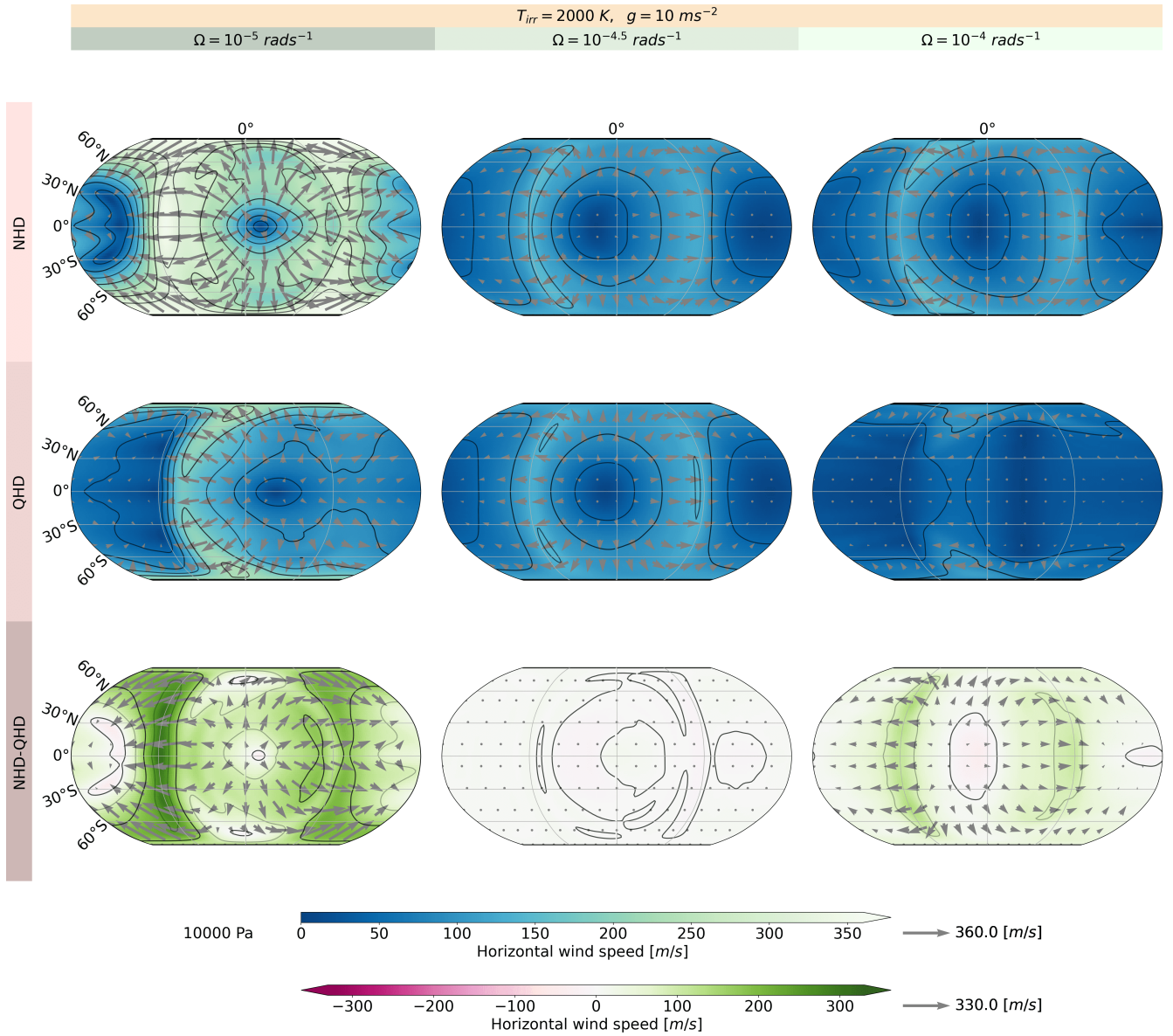


Figure 6. Divergent component of the Helmholtz decomposition at $10'000 \text{ Pa}$ for the NHD and QHD equation sets with $g = 10 \text{ ms}^{-2}$, $T_{irr} = 2'000 \text{ K}$ and with altering Ω .

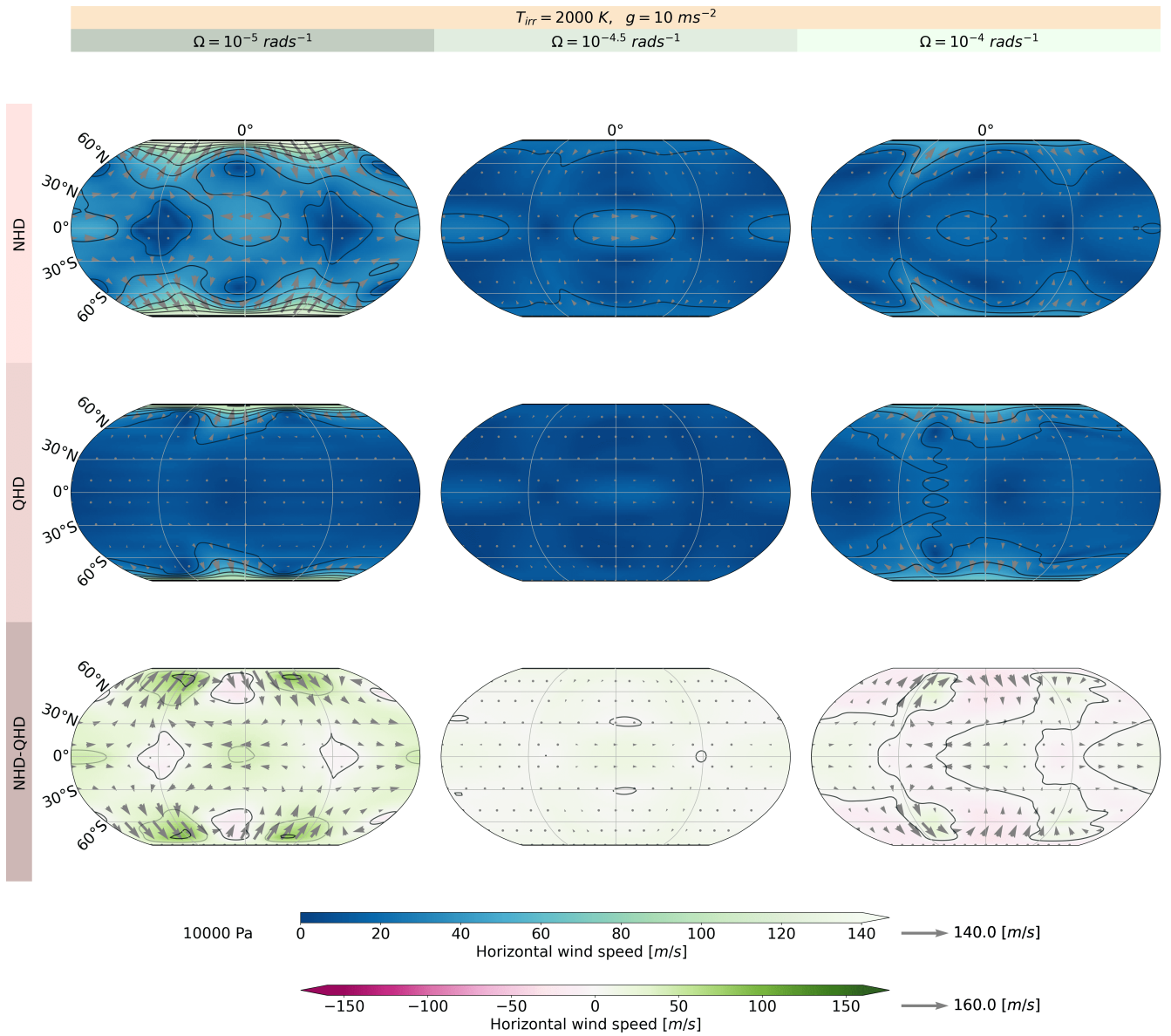


Figure 7. Rotational eddy component of the Helmholtz decomposition at 10'000 Pa for the NHD and QHD equation sets with $g = 10 \text{ ms}^{-2}$, $T_{irr} = 2'000 \text{ K}$ and with altering Ω .

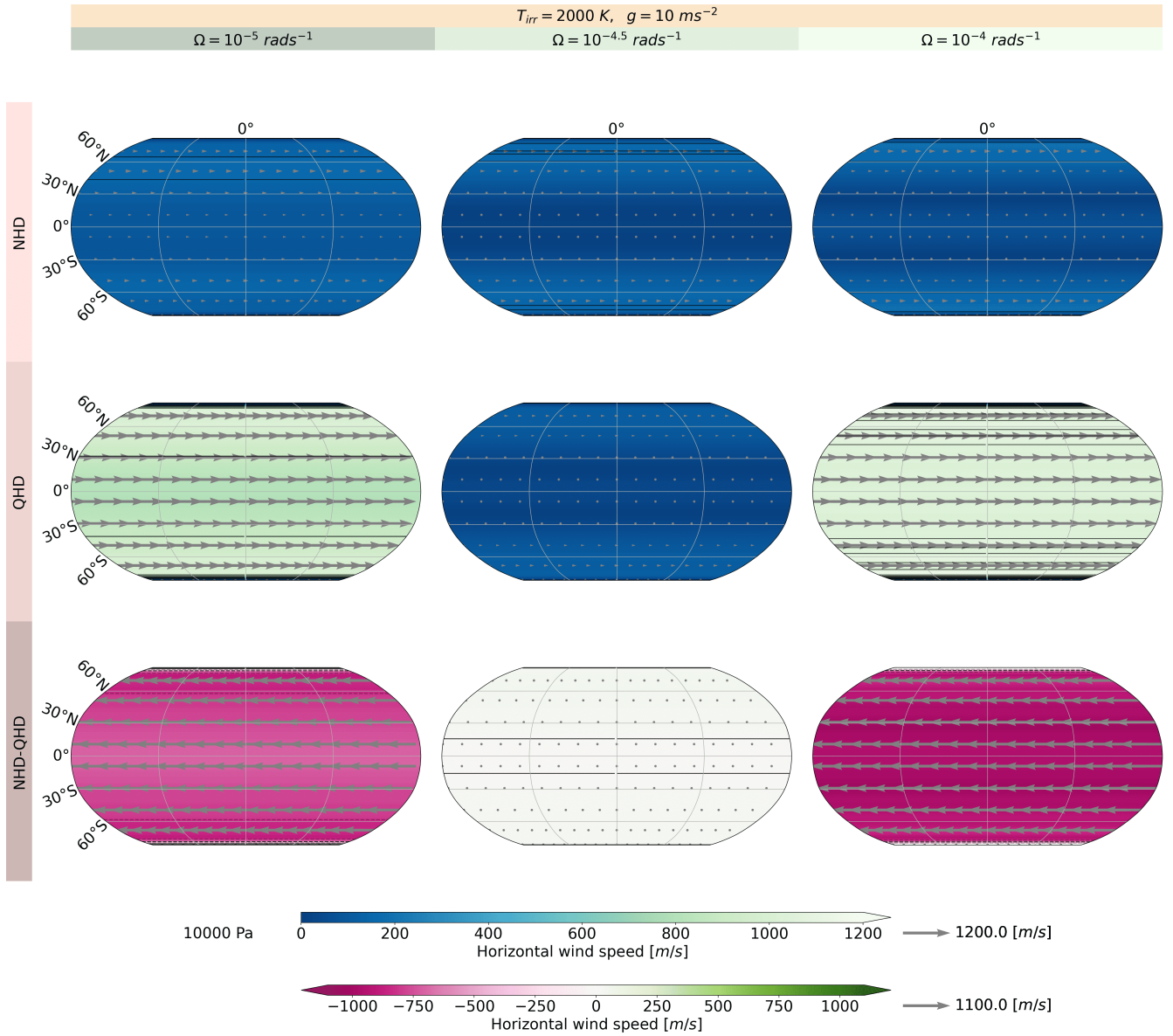


Figure 8. Rotational jet component of the Helmholtz decomposition at $10'000 \text{ Pa}$ for the NHD and QHD equation sets with $g = 10 \text{ ms}^{-2}$, $T_{irr} = 2'000 \text{ K}$ and with altering Ω .

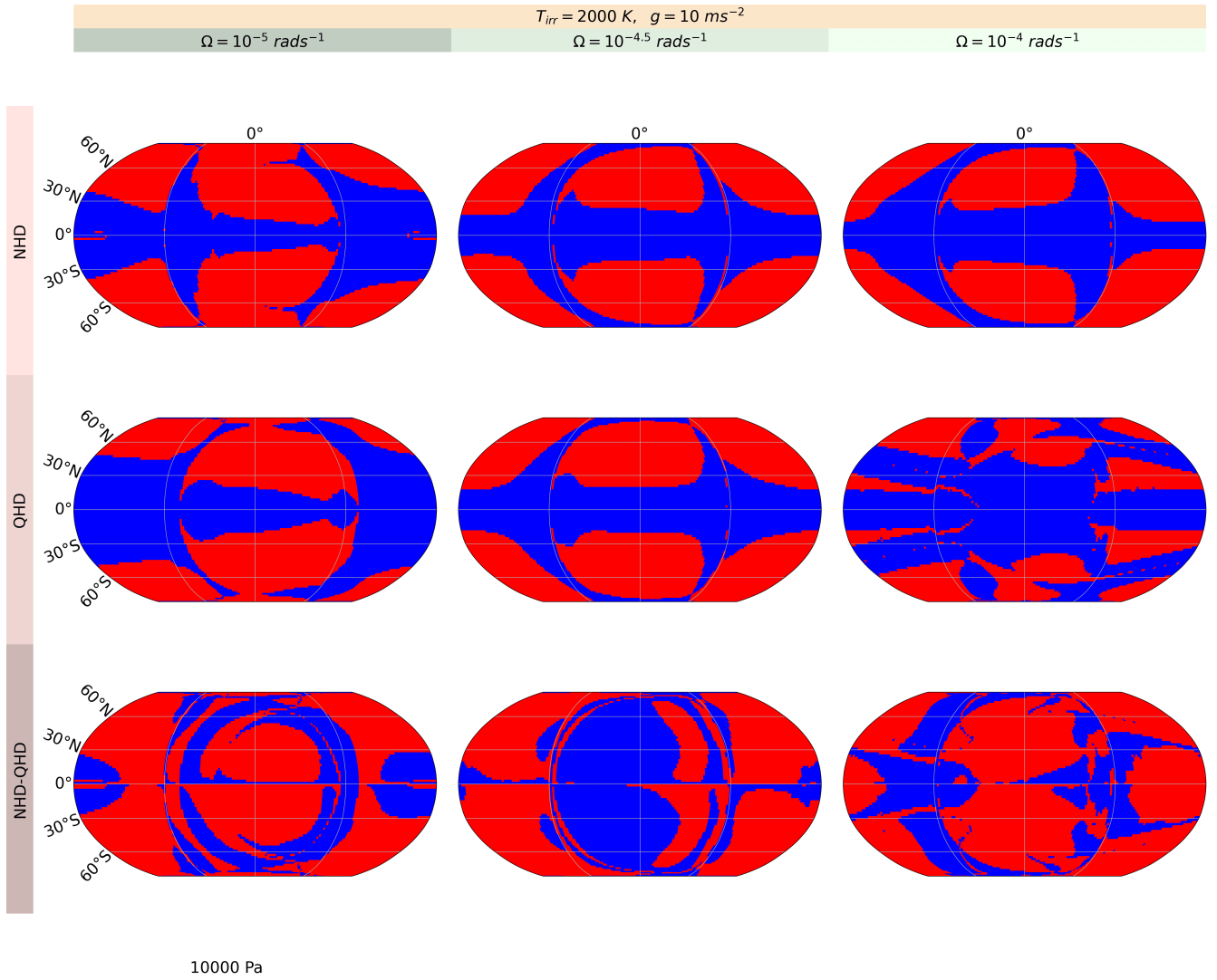


Figure 9. Sign of $\frac{v \tan(\Phi)}{10w} - 1$ at 10'000 Pa for the NHD and QHD equation sets with $g = 10 \text{ ms}^{-2}$, $T_{irr} = 2'000 \text{ K}$ and with altering Ω . Dark blue and bright blue regions show negative and positive values

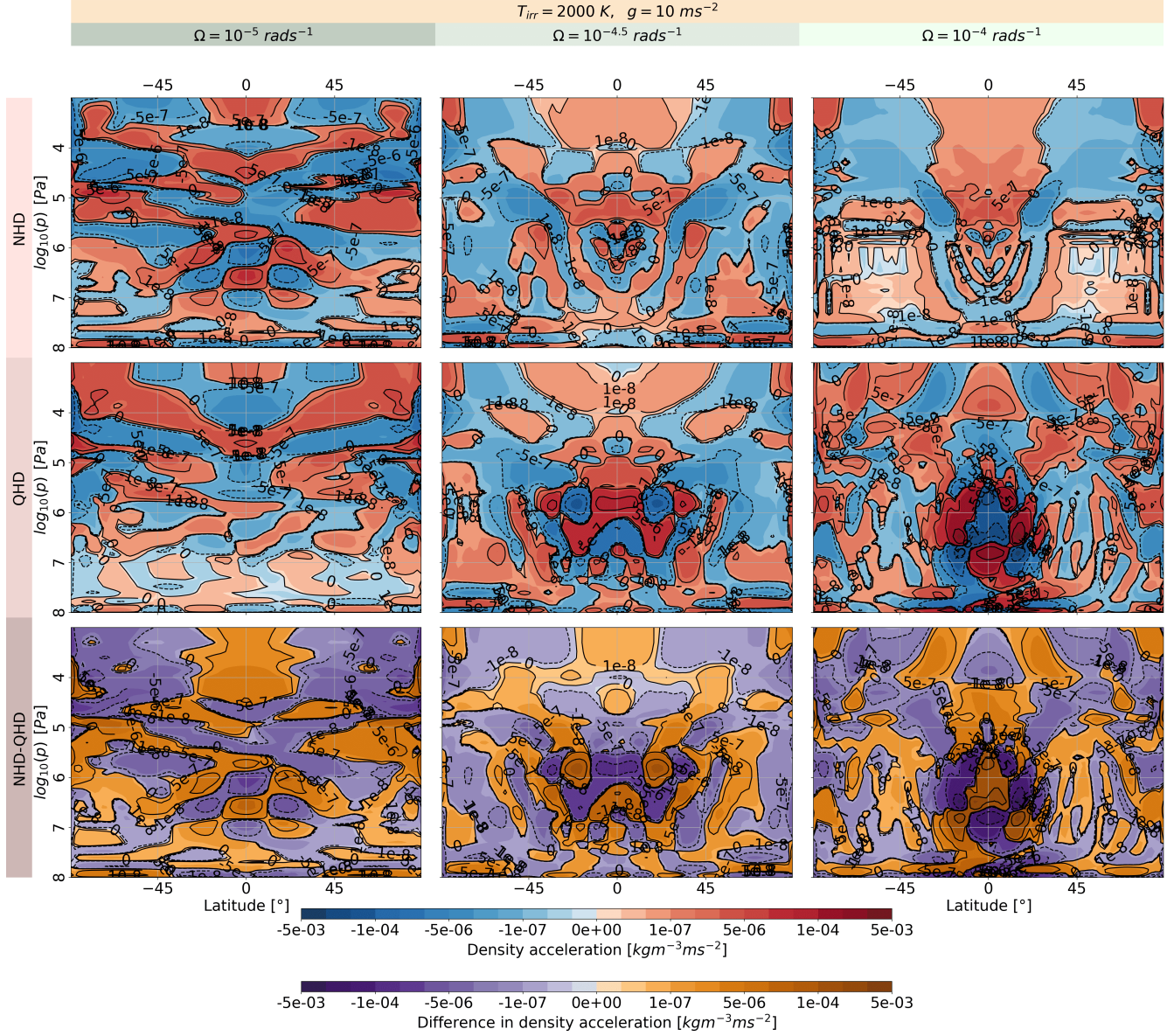


Figure 10. Horizontal acceleration for the NHD and QHD equation sets with $g = 10 \text{ ms}^{-2}$, $T_{irr} = 2'000 \text{ K}$ and with altering Ω .

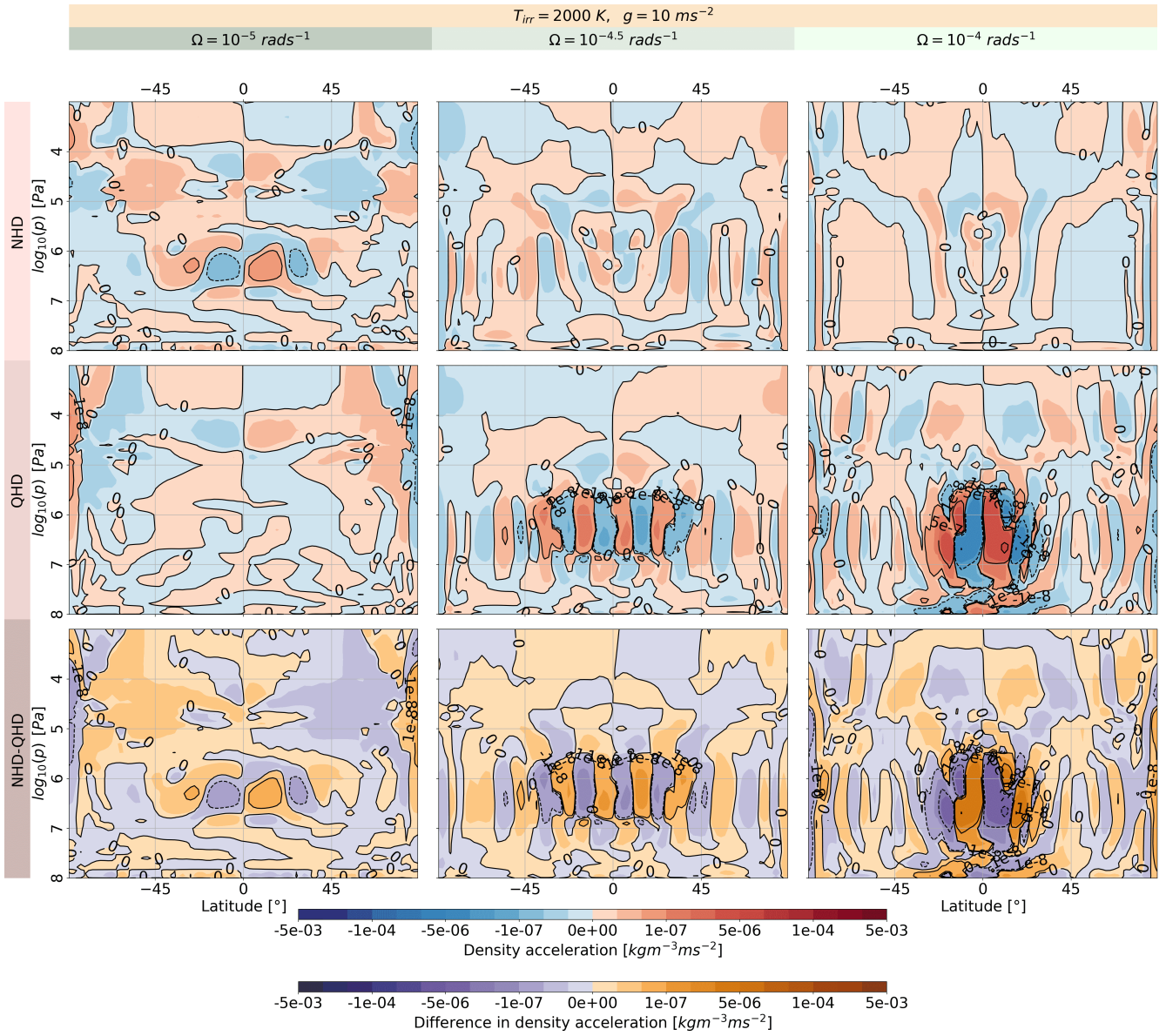


Figure 11. Vertical acceleration for the NHD and QHD equation sets with $g = 10 \text{ ms}^{-2}$, $T_{irr} = 2'000 \text{ K}$ and with altering Ω .

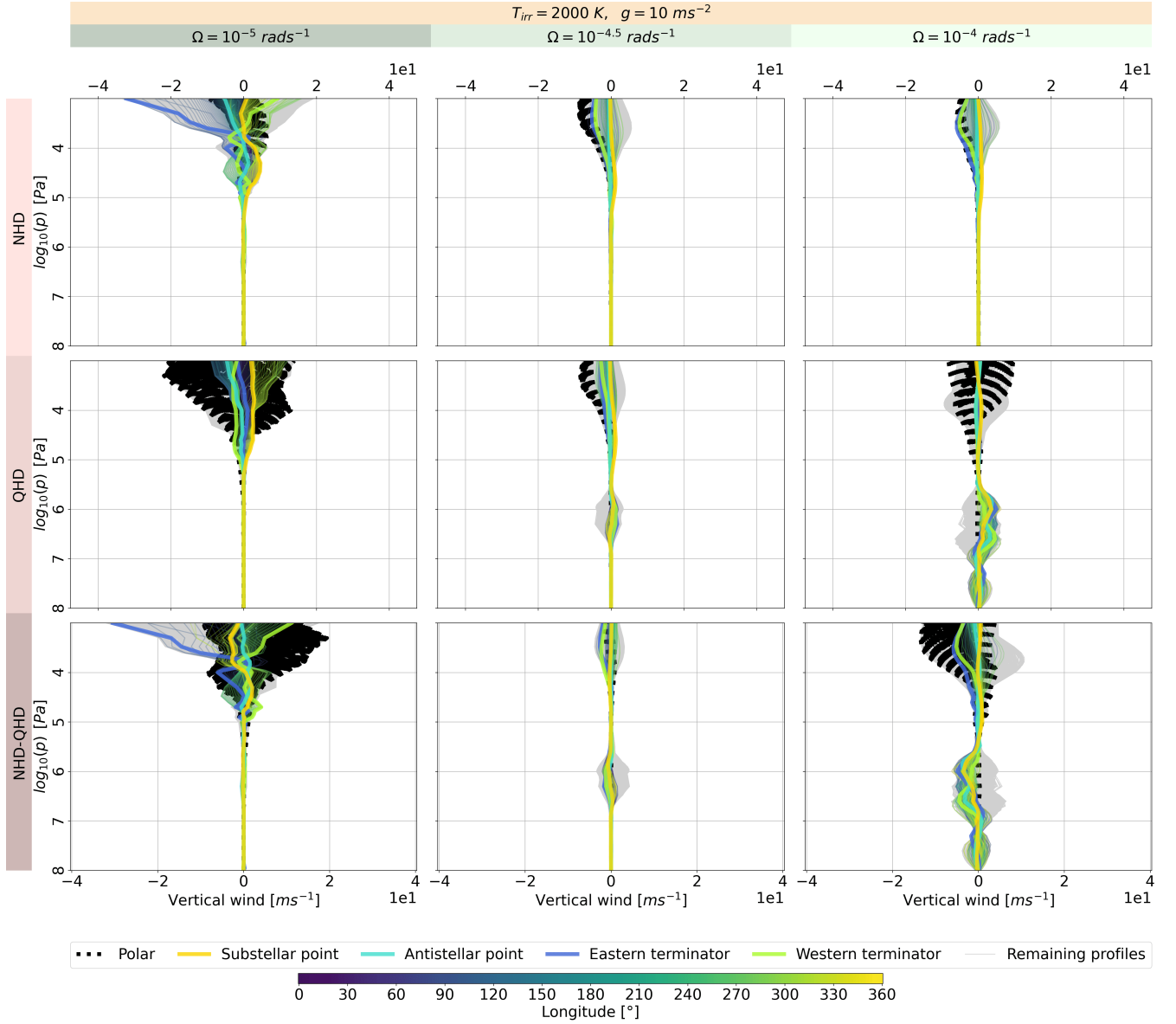


Figure 12. Vertical wind speed at each grid point for the NHD and QHD equation sets with $g = 10 \text{ ms}^{-2}$, $T_{irr} = 2'000 \text{ K}$ and with altering Ω . The coloured lines indicate momenta profiles along the equator and its coordinates by the colourbar. The dotted black thin line shows momenta profiles at the latitudes 87°N and 87°S . The bold coloured lines represent momenta profiles at the western, eastern terminators, sub- and antistellar point. The grey lines represents all the other momenta profiles.

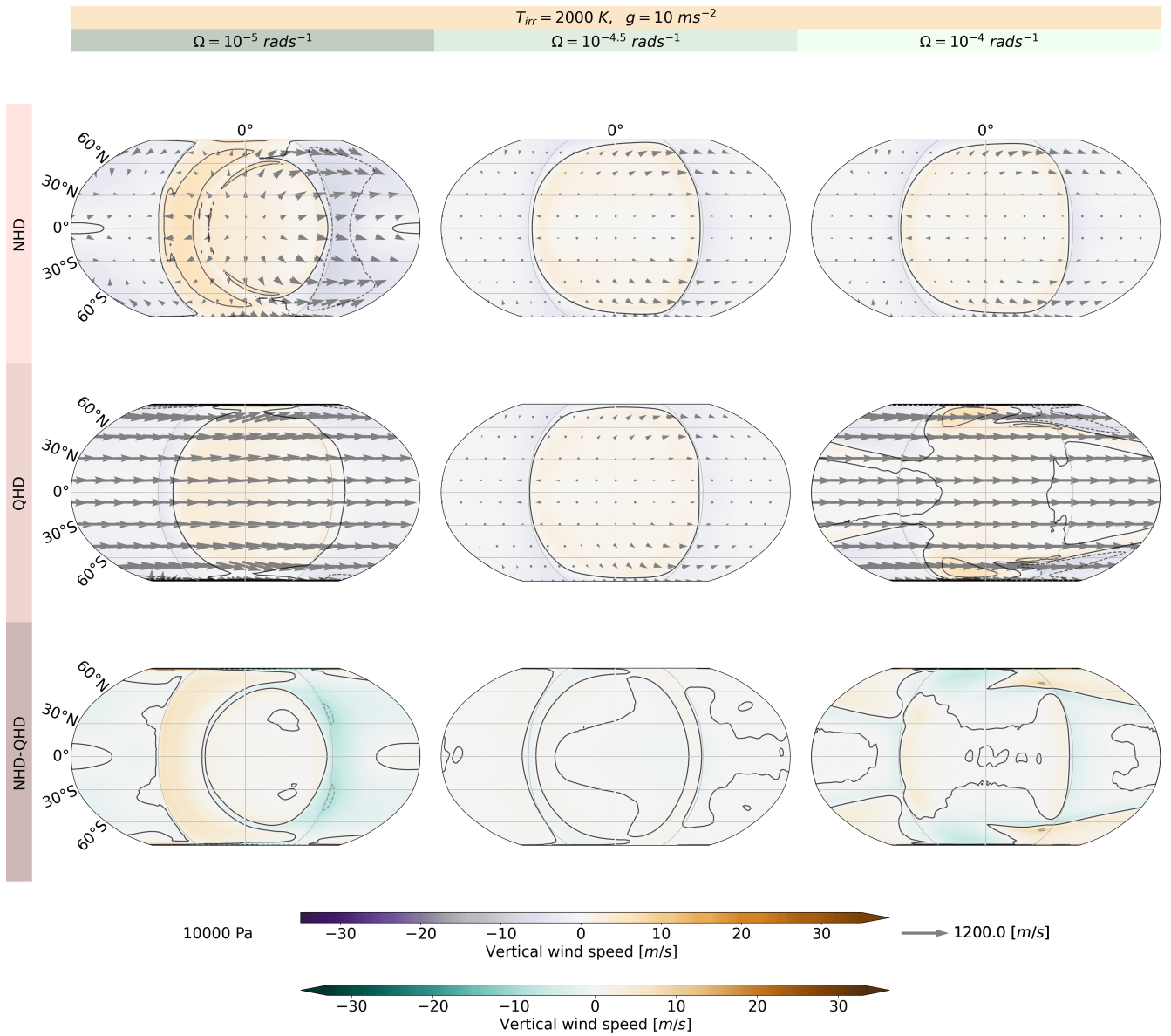


Figure 13. Vertical wind speed at $10'000 \text{ Pa}$ for the NHD and QHD equation sets with $g = 10 \text{ ms}^{-2}$, $T_{irr} = 2'000 \text{ K}$ and with altering Ω . The arrows indicate the horizontal wind speed

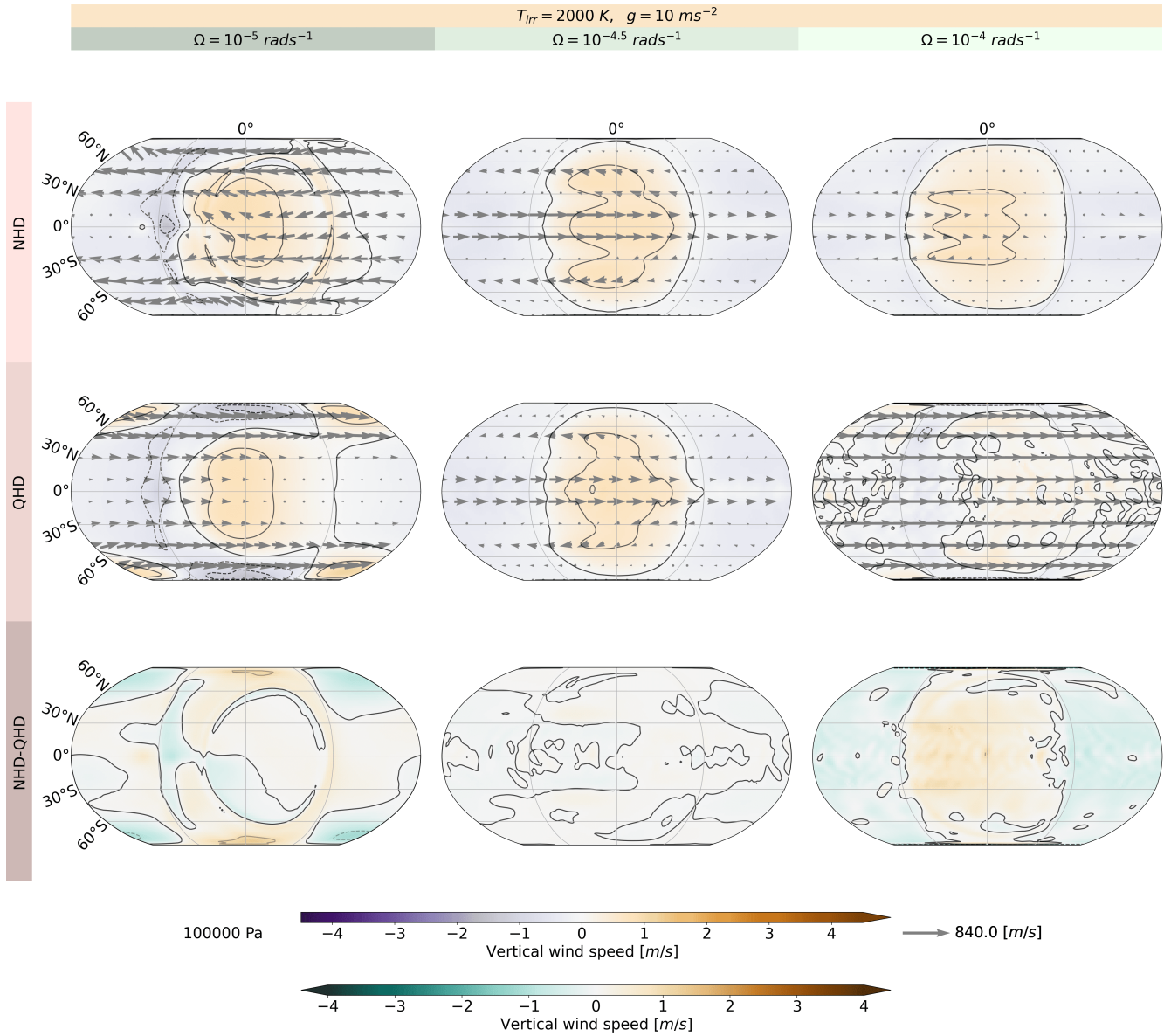


Figure 14. Vertical wind speed at 100'000 Pa for the NHD and QHD equation sets with $g = 10 \text{ ms}^{-2}$, $T_{irr} = 2'000 \text{ K}$ and with altering Ω . The arrows indicate the horizontal wind speed

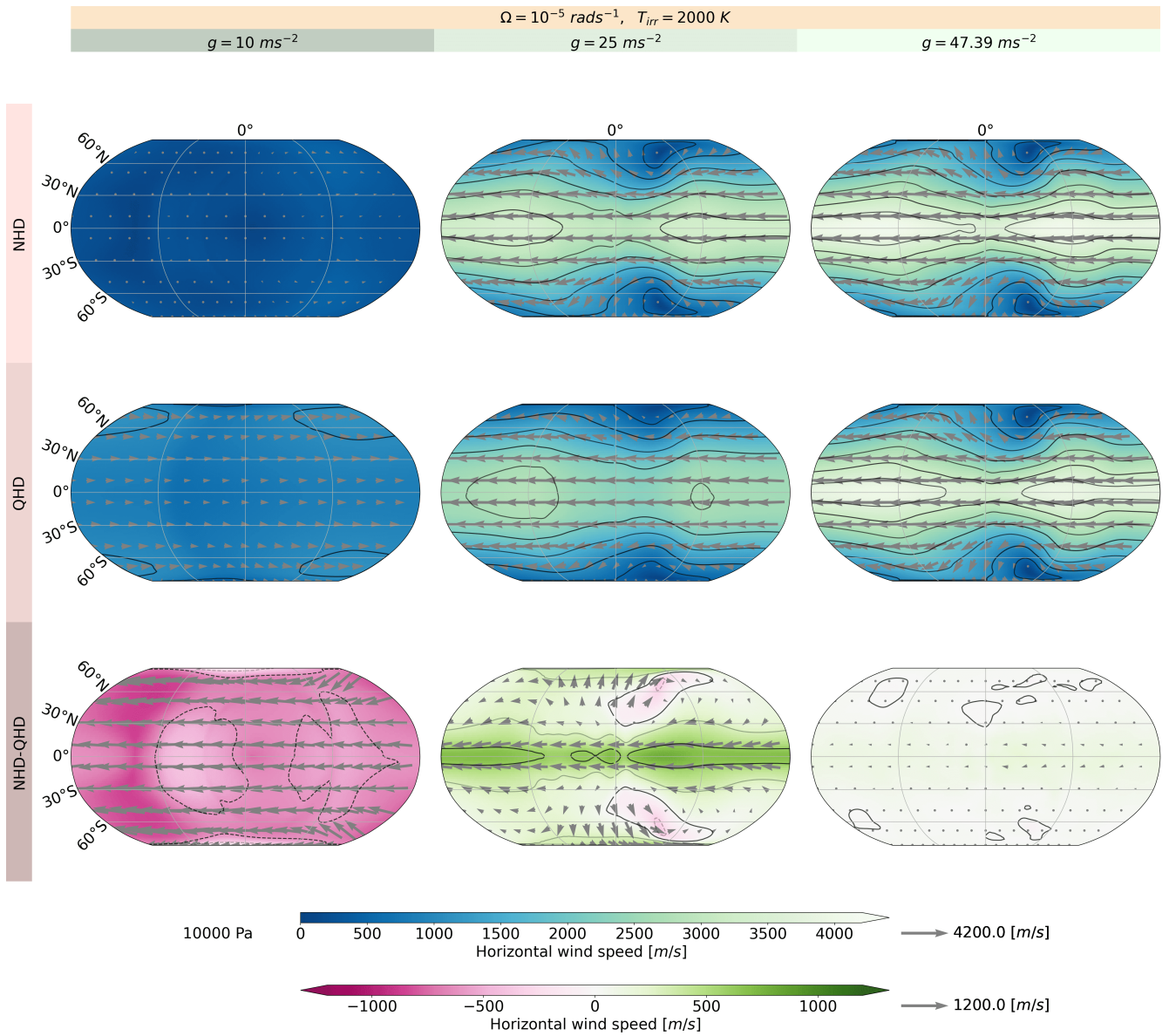


Figure 15. Horizontal wind speed at 10'000 Pa for the NHD and QHD equation sets with $\Omega = 1 \cdot 10^{-5} \text{ rad/s}$, $T_{irr} = 2'000 \text{ K}$ and with altering g .

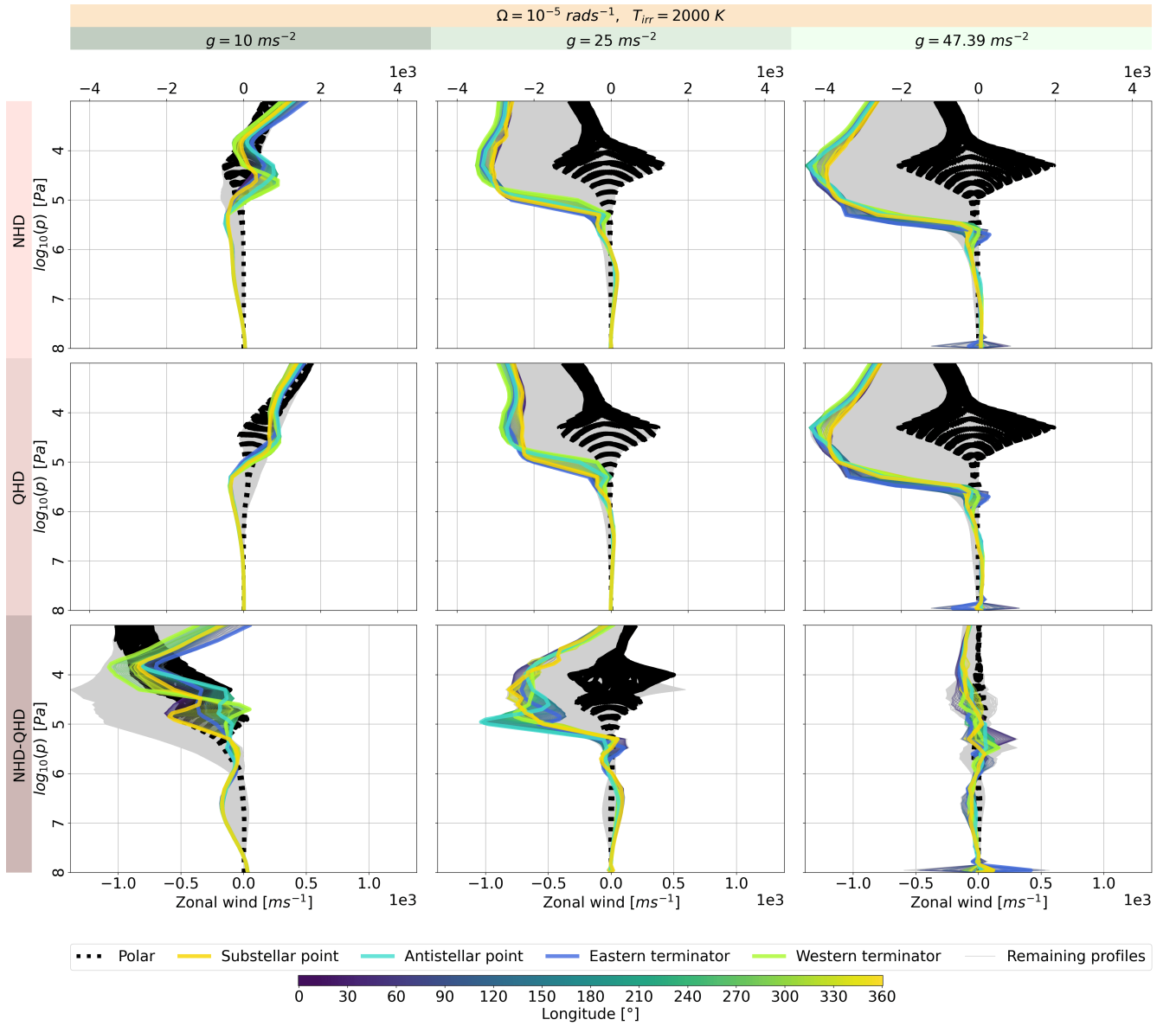


Figure 16. Zonal wind speed at each grid point for the NHD and QHD equation sets with $\Omega = 1 \cdot 10^{-5} \text{ rad/s}$, $T_{irr} = 2'000 \text{ K}$ and with altering g . The coloured lines indicate momenta profiles along the equator and its coordinates by the colourbar. The dotted black thin line shows momenta profiles at the latitudes 87°N and 87°S . The bold coloured lines represent momenta profiles at the western, eastern terminators, sub- and antistellar point. The grey lines represents all the other momenta profiles.

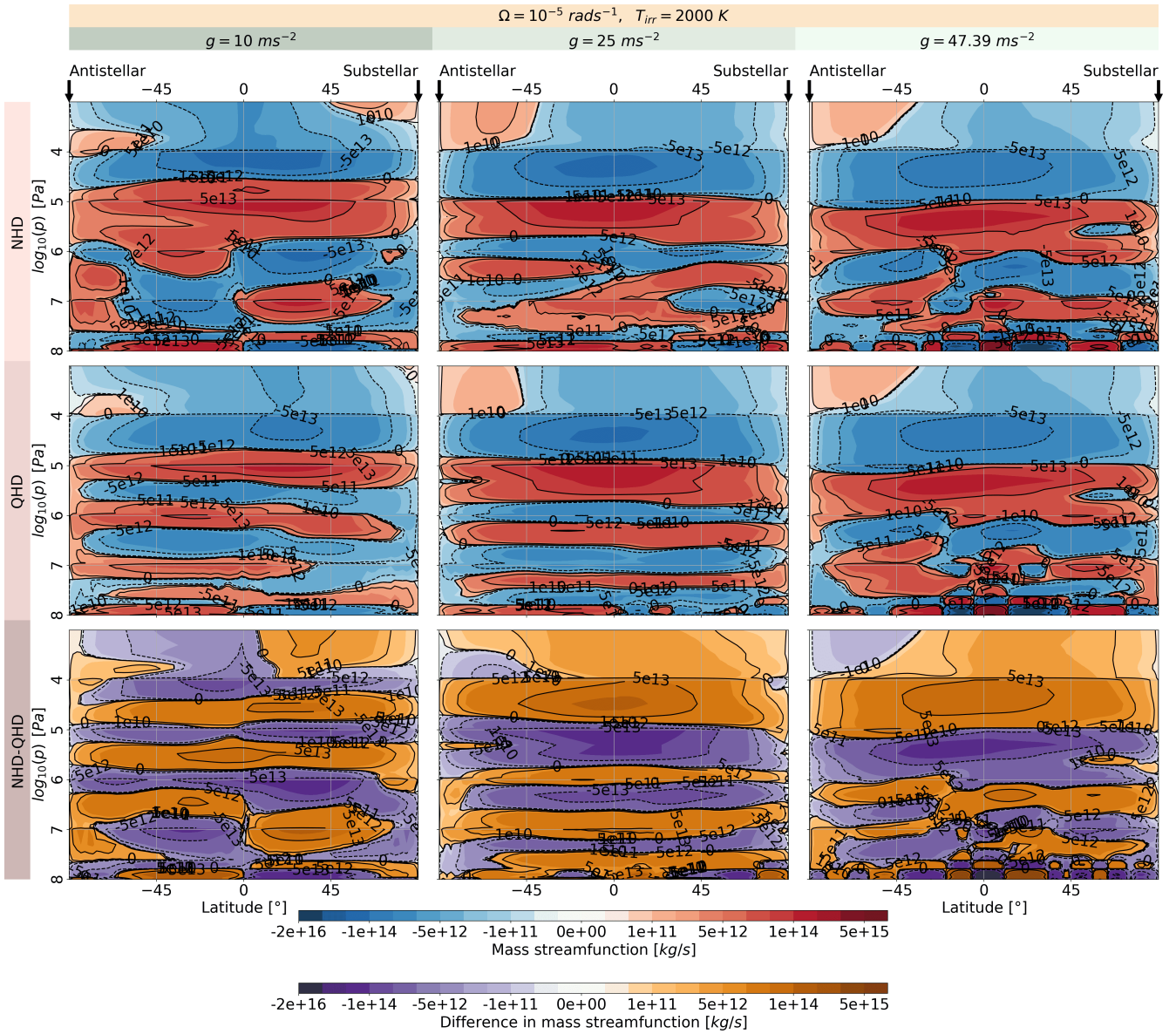


Figure 17. Overturning circulation depicted by the streamfunction Ψ' in tidally locked coordinates for the NHD and QHD equation sets with $\Omega = 1 \cdot 10^{-5} \text{ rad/s}$, $T_{\text{irr}} = 2'000 \text{ K}$ and with altering g .

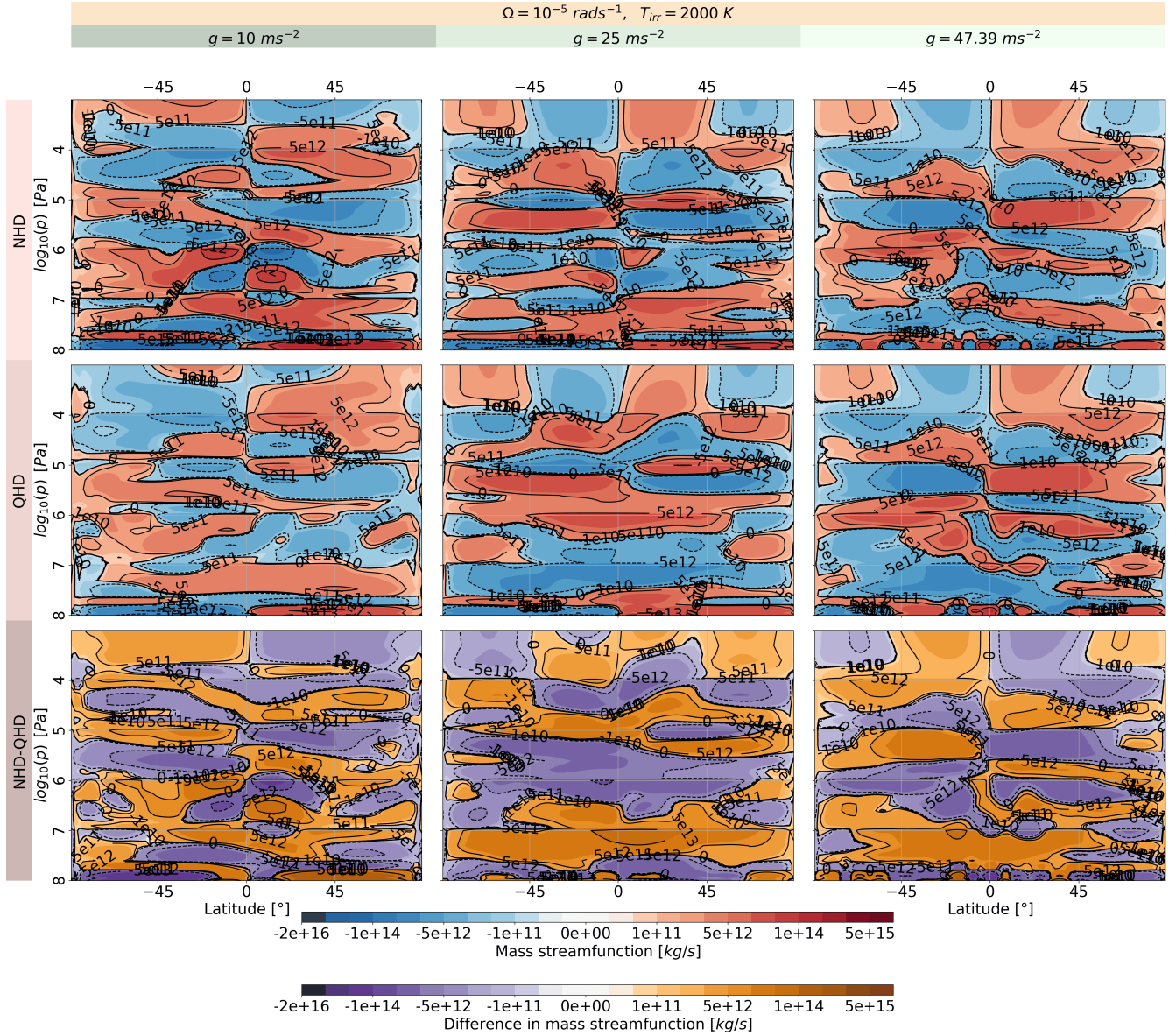


Figure 18. Overturning circulation depicted by the streamfunction Ψ for the NHD and QHD equation sets with $\Omega = 1 \cdot 10^{-5} \text{ rad/s}$, $T_{\text{irr}} = 2'000 \text{ K}$ and with altering g .

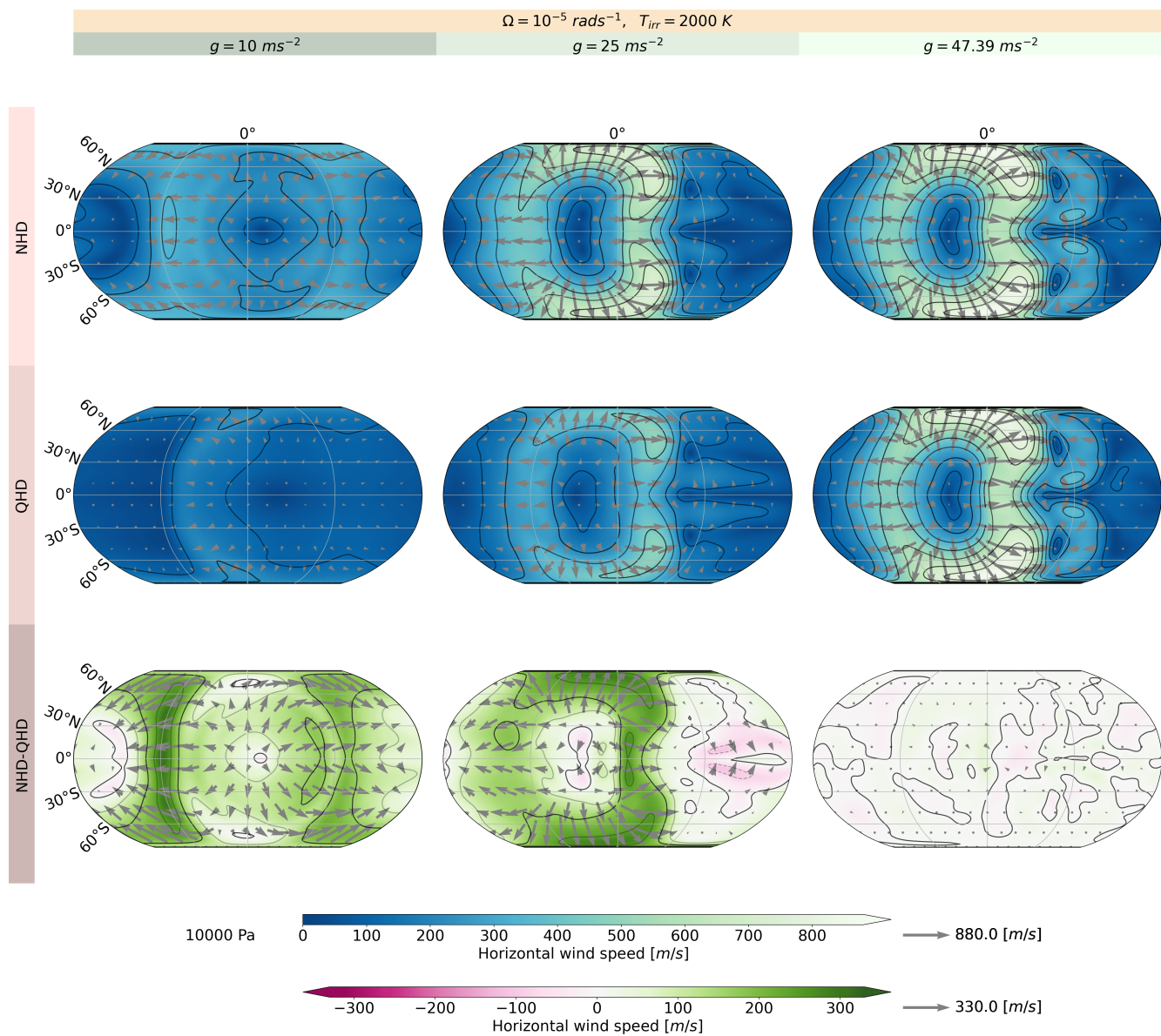


Figure 19. Divergent component of the Helmholtz decomposition at $10'000 \text{ Pa}$ for the NHD and QHD equation sets with $\Omega = 1 \cdot 10^{-5} \text{ rad/s}$, $T_{irr} = 2'000 \text{ K}$ and with altering g .

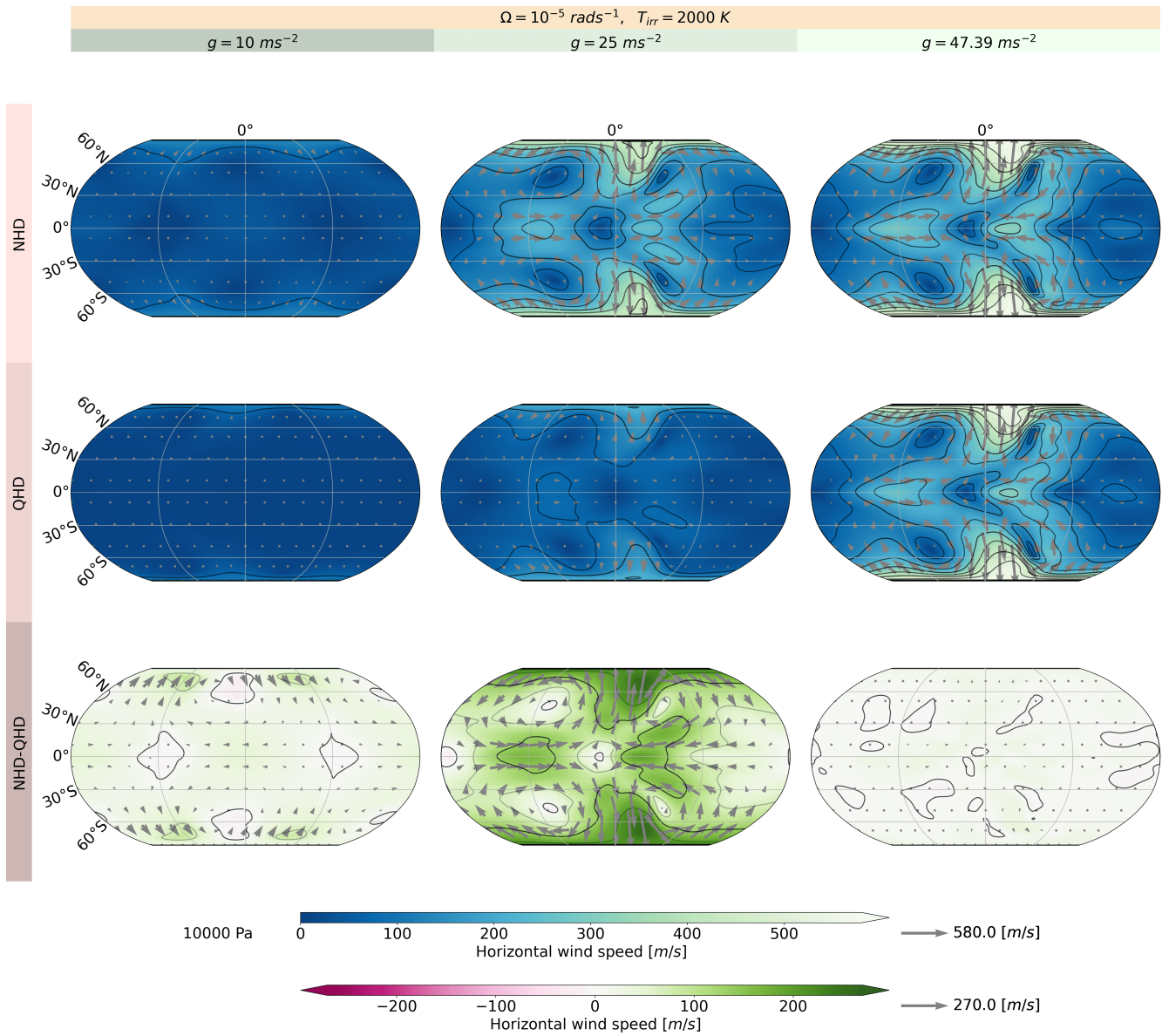


Figure 20. Rotational eddy component of the Helmholtz decomposition at 10'000 Pa for the NHD and QHD equation sets with $\Omega = 1 \cdot 10^{-5} \text{ rad/s}$, $T_{\text{irr}} = 2'000 \text{ K}$ and with altering g .

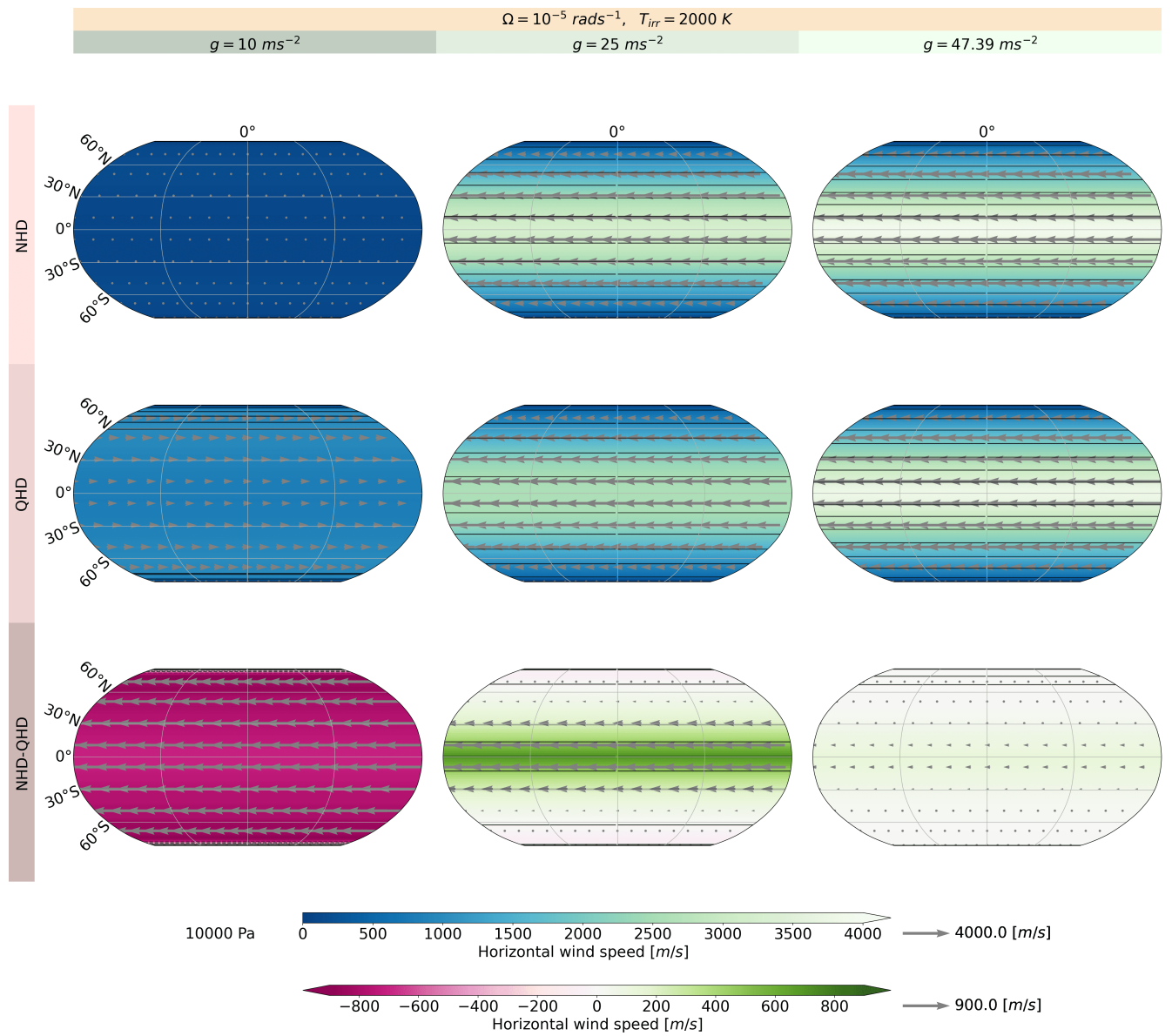


Figure 21. Rotational jet component of the Helmholtz decomposition at $10'000 \text{ Pa}$ for the NHD and QHD equation sets with $\Omega = 1 \cdot 10^{-5} \text{ rad/s}$, $T_{\text{irr}} = 2'000 \text{ K}$ and with altering g .

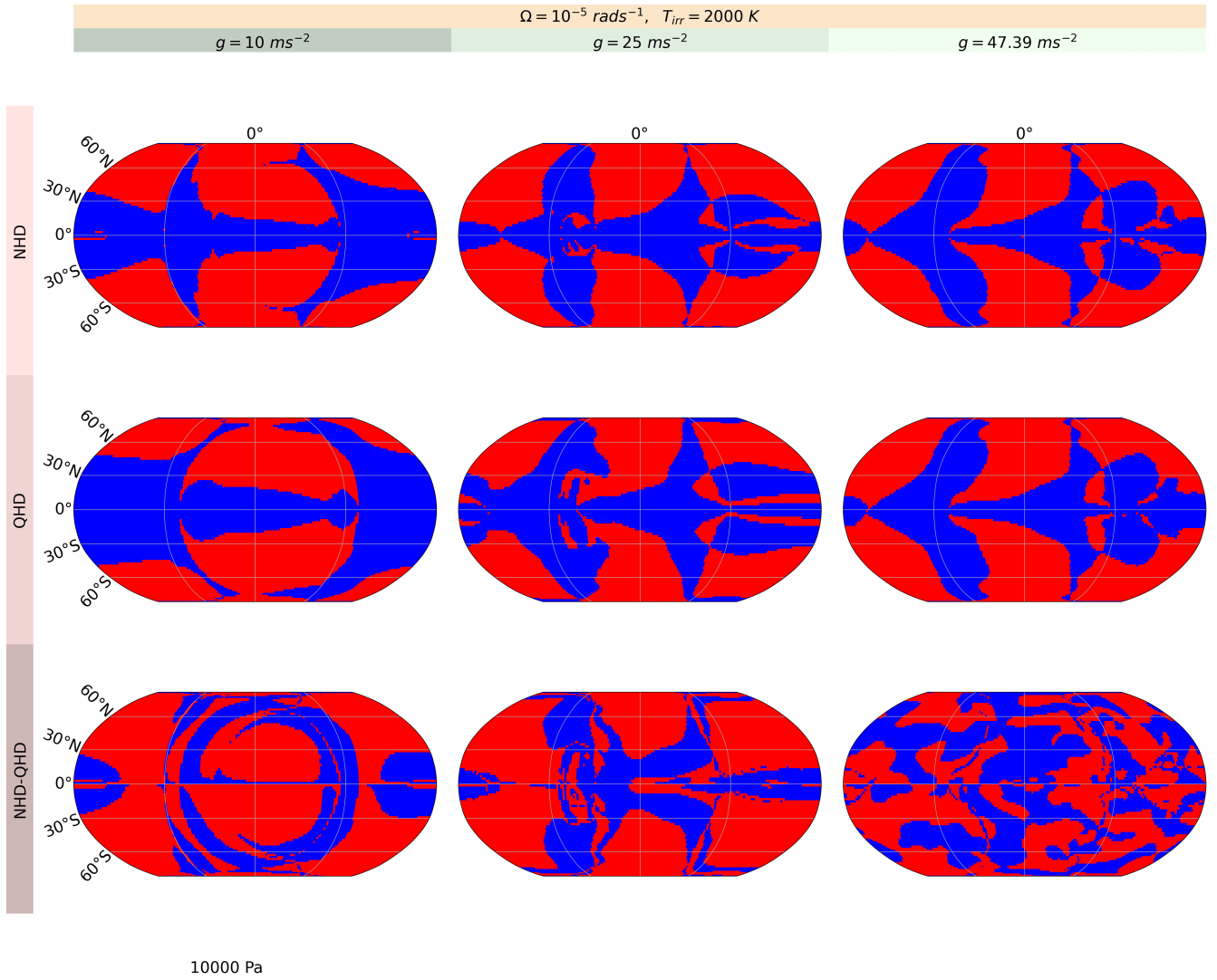


Figure 22. Sign of $\frac{v \tan(\Phi)}{10w} - 1$ for the NHD and QHD equation sets with $\Omega = 1 \cdot 10^{-5} \text{ rad/s}$, $T_{irr} = 2'000 \text{ K}$ and with altering g . Dark blue and bright blue regions show negative and positive values

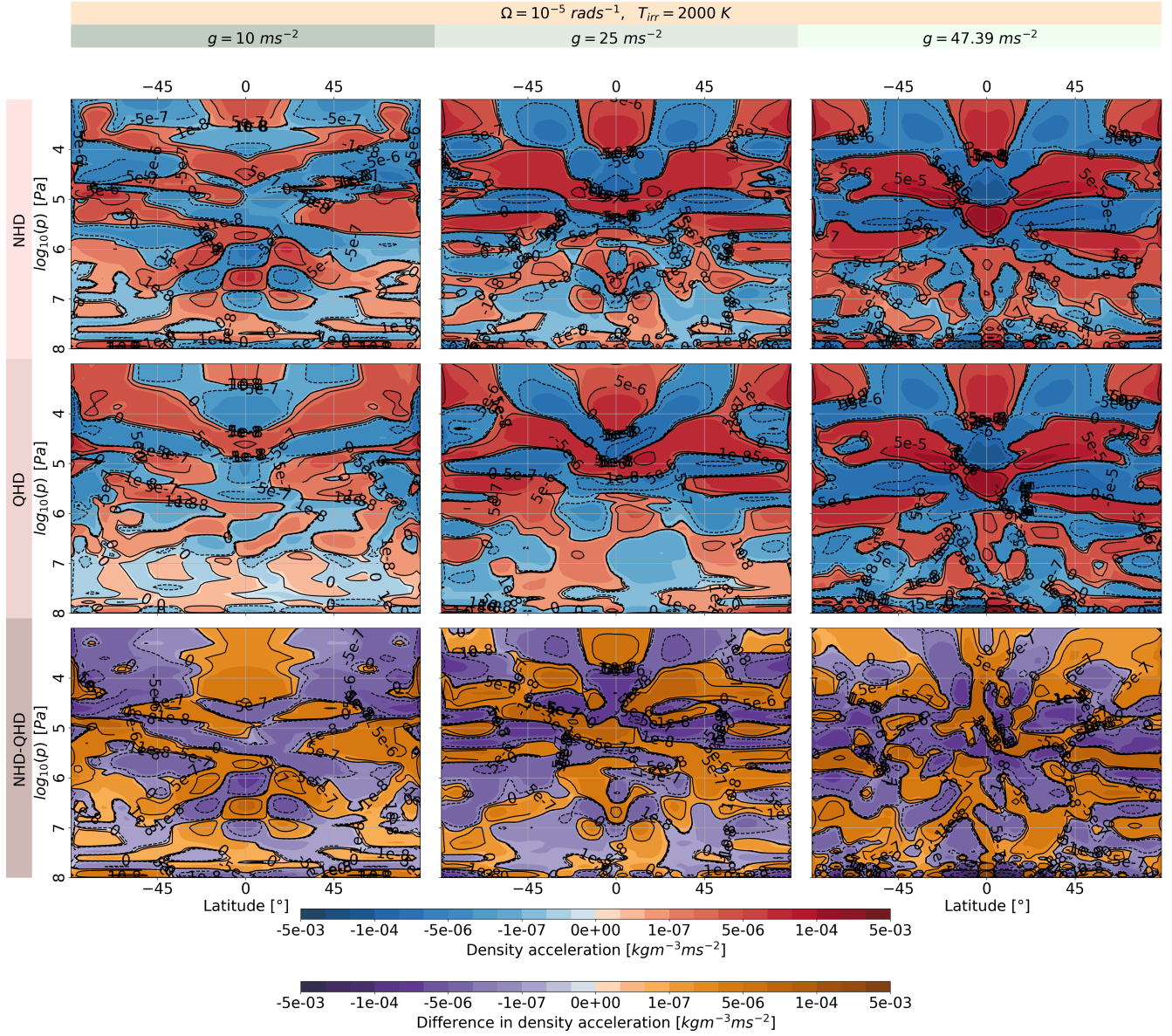


Figure 23. Horizontal acceleration for the NHD and QHD equation sets with $\Omega = 1 \cdot 10^{-5} \text{ rad/s}$, $T_{\text{irr}} = 2'000 \text{ K}$ and with altering g .

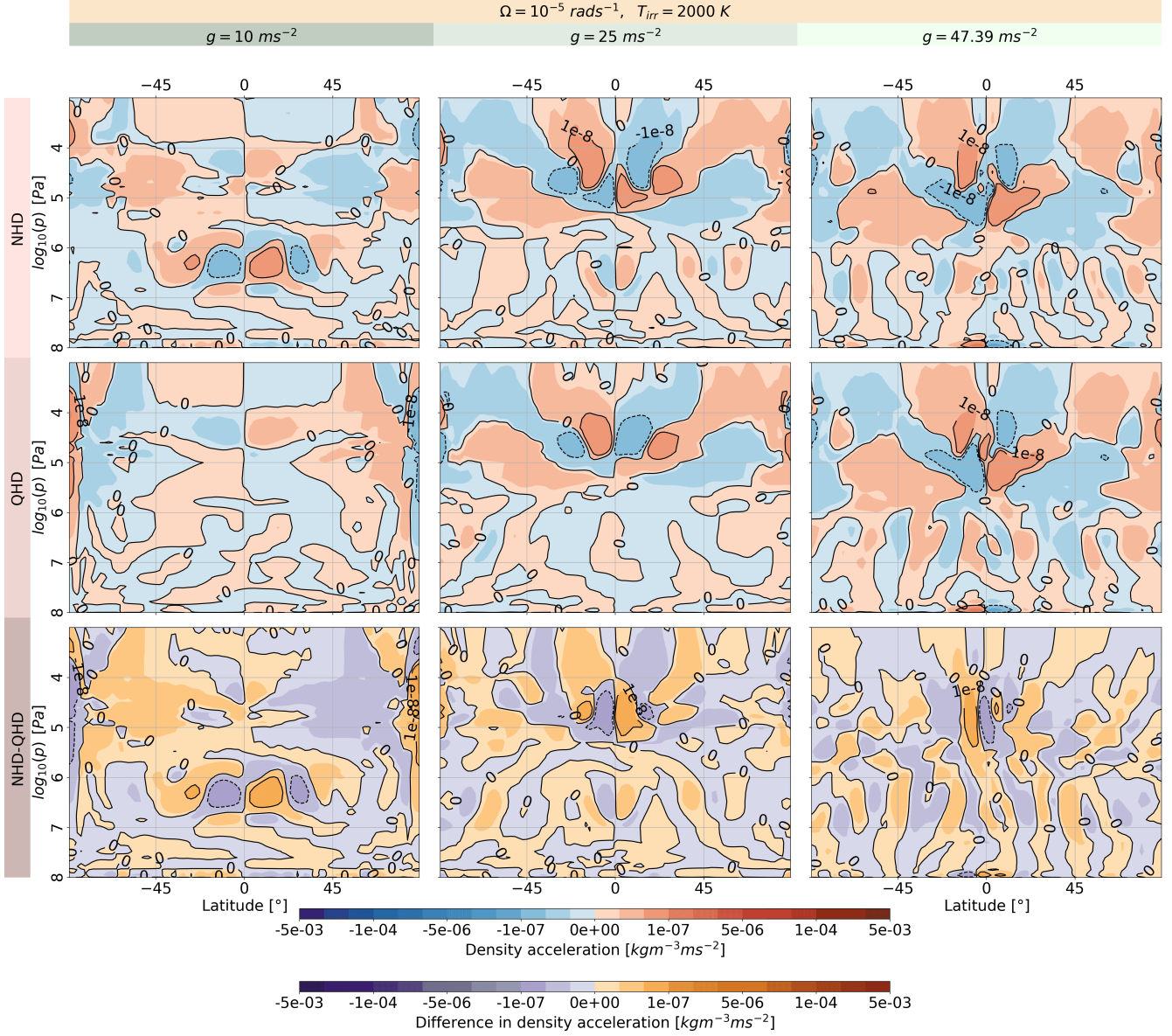


Figure 24. Vertical acceleration for the NHD and QHD equation sets with $\Omega = 1 \cdot 10^{-5} \text{ rad/s}$, $T_{\text{irr}} = 2'000 \text{ K}$ and with altering g .

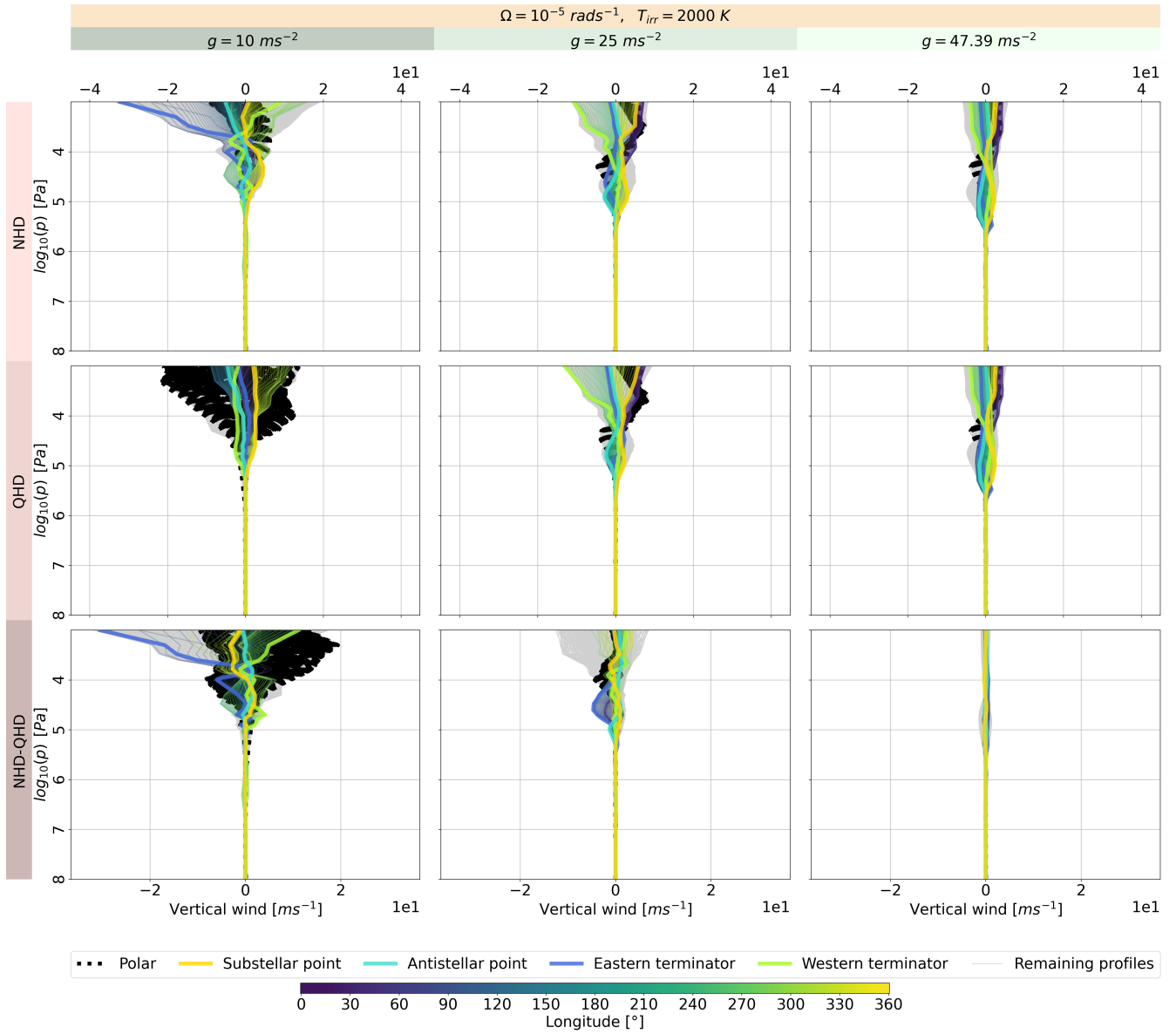


Figure 25. Vertical wind speed at each grid point for the NHD and QHD equation sets with $\Omega = 1 \cdot 10^{-5} \text{ rad/s}$, $T_{irr} = 2'000 \text{ K}$ and with altering g . The coloured lines indicate momenta profiles along the equator and its coordinates by the colourbar. The dotted black thin line shows momenta profiles at the latitudes 87°N and 87°S . The bold coloured lines represent momenta profiles at the western, eastern terminator, sub- and antistellar point. The grey lines represent all the other momenta profiles.

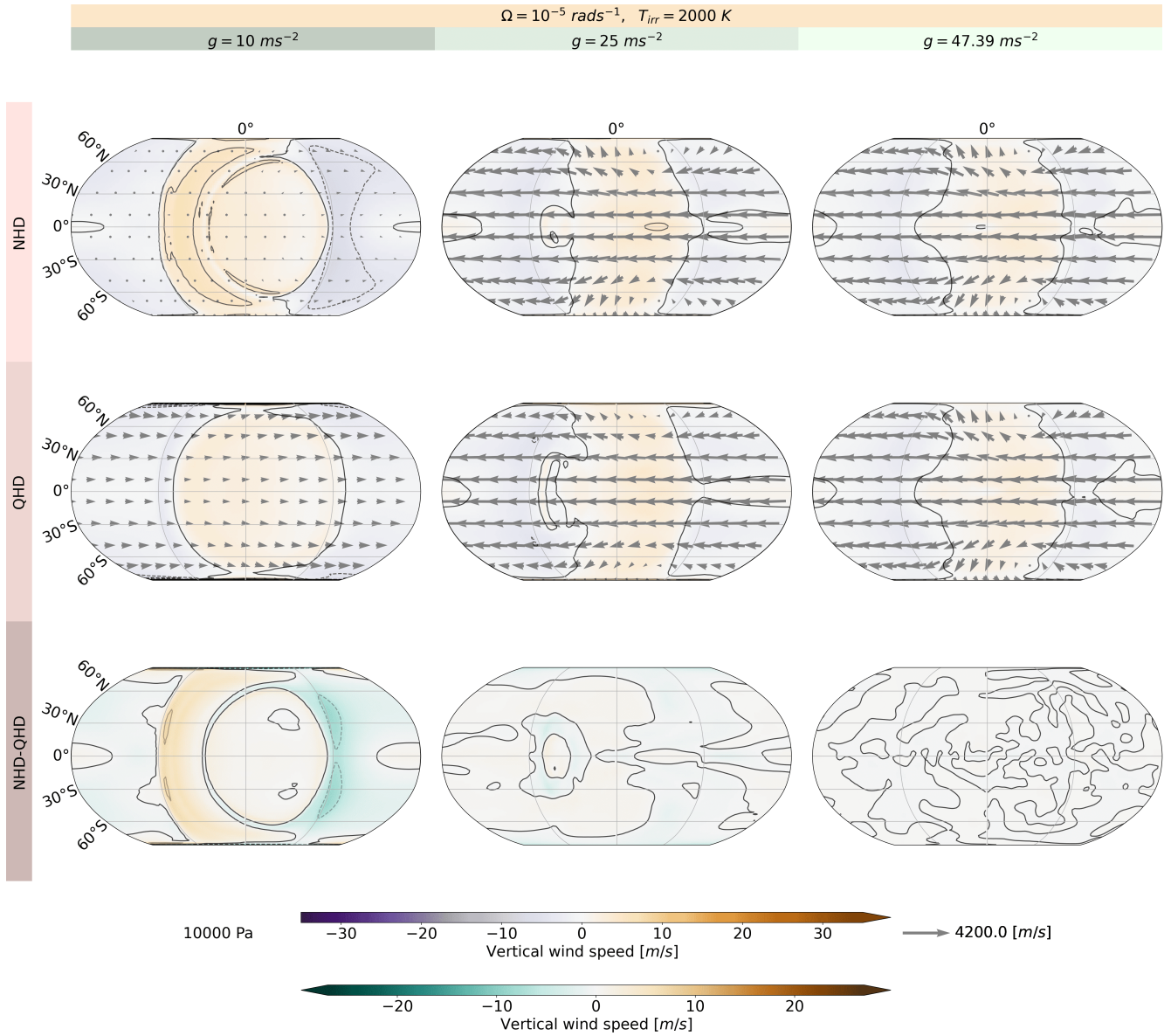


Figure 26. Vertical wind speed at 10'000 Pa for the NHD and QHD equation sets with $\Omega = 1 \cdot 10^{-5} \text{ rad/s}$, $T_{irr} = 2'000 \text{ K}$ and with altering g . The arrows indicate the horizontal wind speed

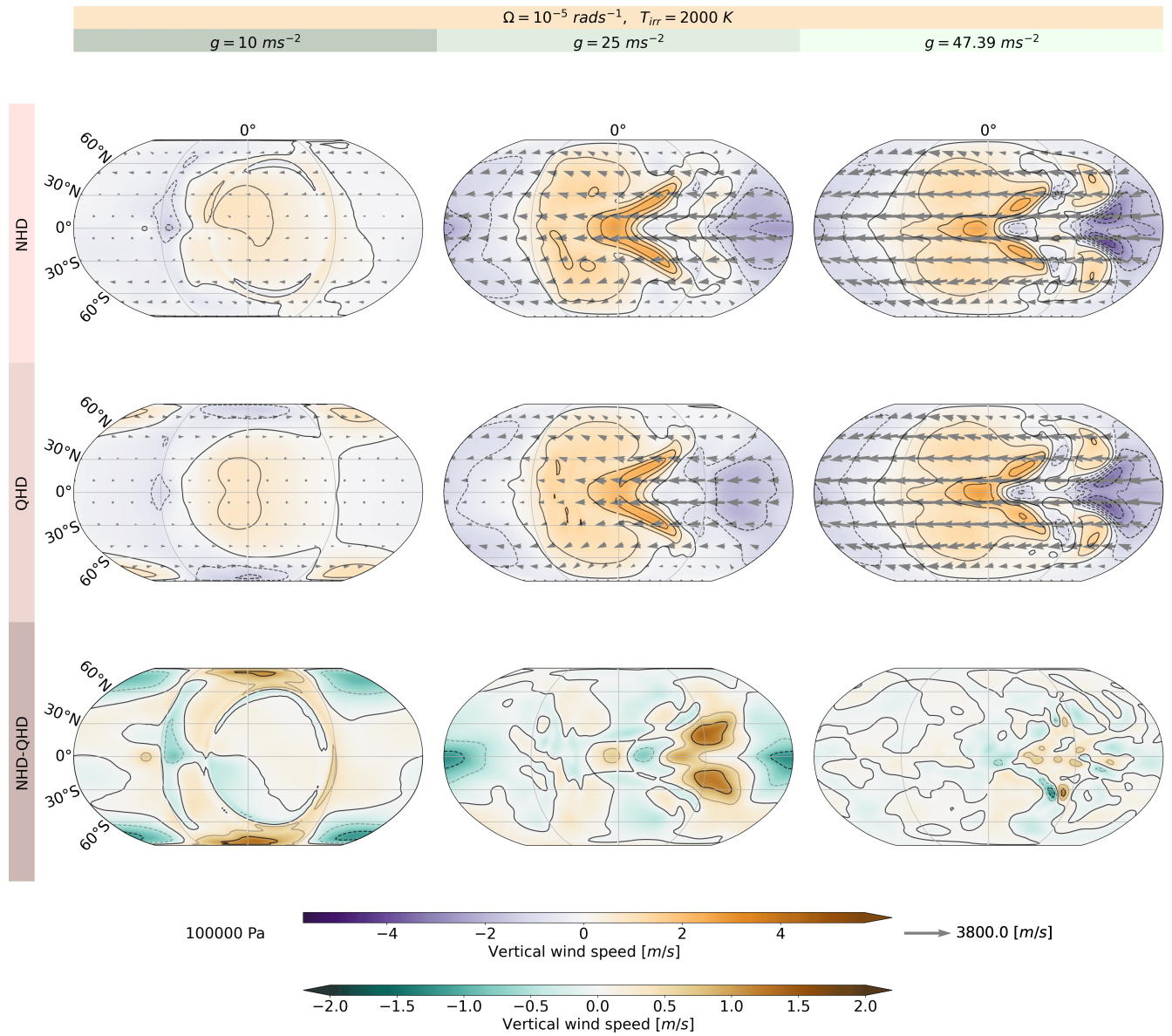


Figure 27. Vertical wind speed at 100'000 Pa for the NHD and QHD equation sets with $\Omega = 1 \cdot 10^{-5} \text{ rad/s}$, $T_{\text{irr}} = 2'000 \text{ K}$ and with altering g . The arrows indicate the horizontal wind speed

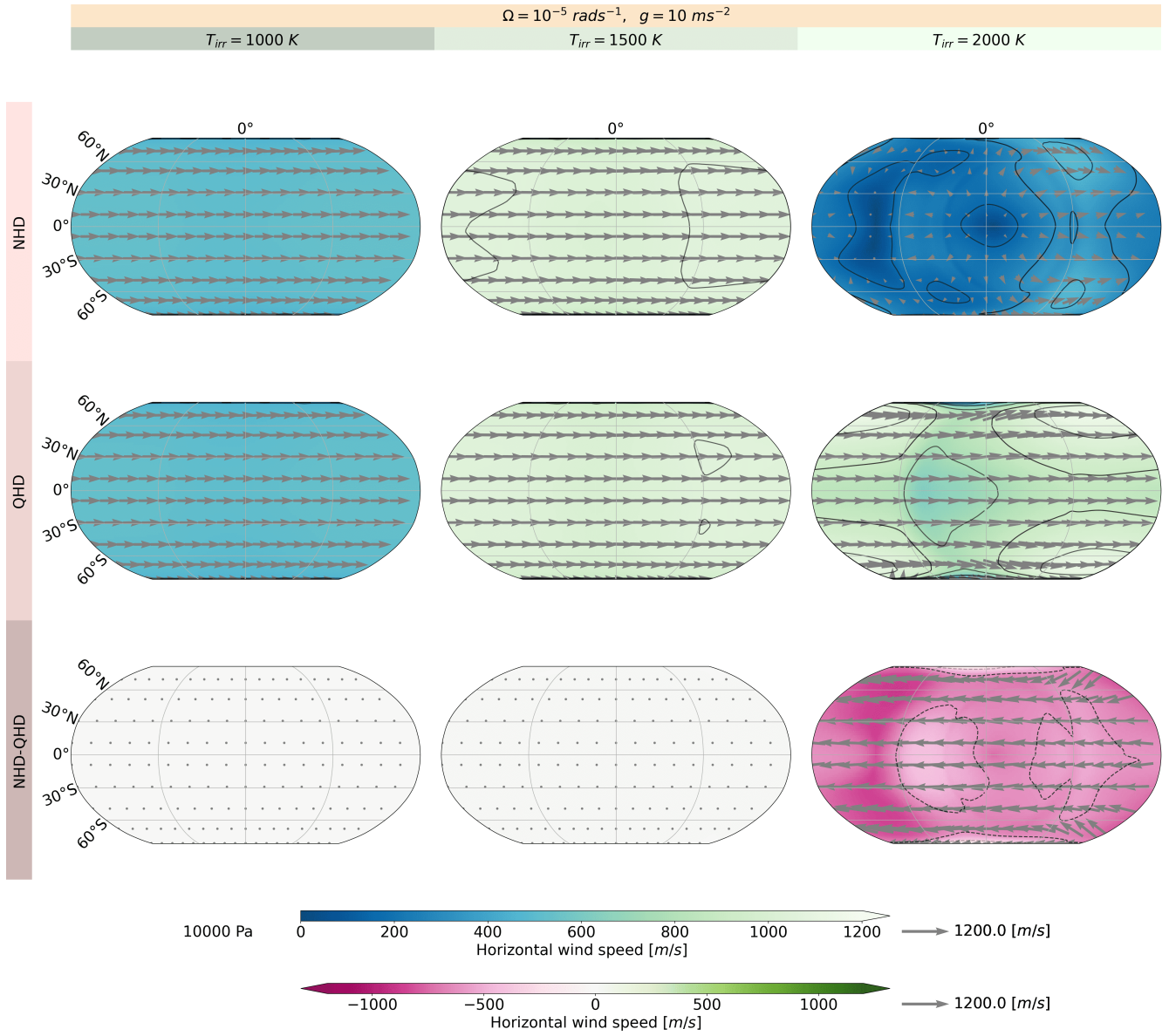


Figure 28. Horizontal wind speed at 10'000 Pa for the NHD and QHD equation sets with $g = 10 \text{ ms}^{-2}$, $\Omega = 1 \cdot 10^{-5} \text{ rad/s}$ and with altering T_{irr} .

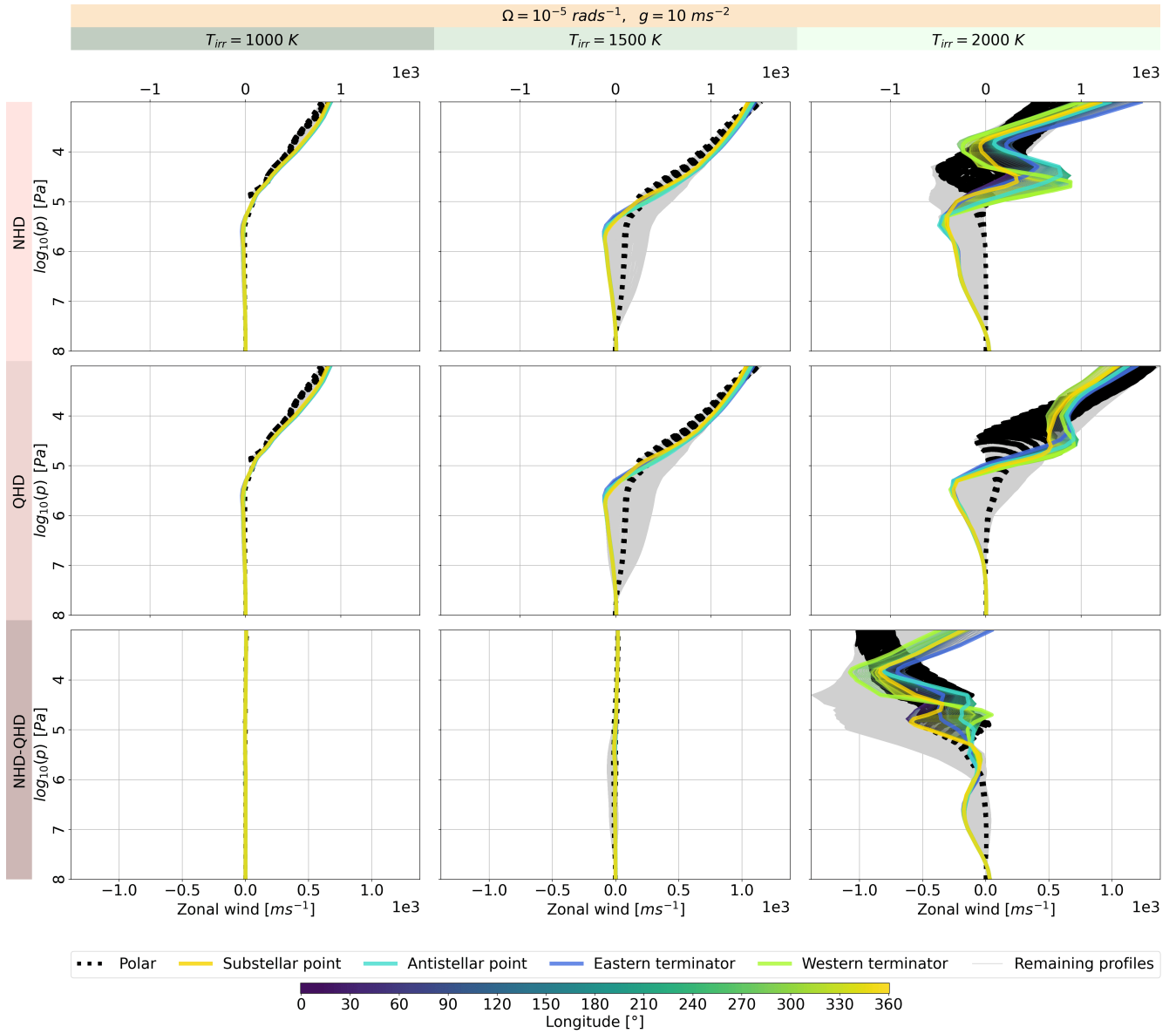


Figure 29. Zonal wind speed at each grid point for the NHD and QHD equation sets with $g = 10 \text{ ms}^{-2}$, $\Omega = 1 \cdot 10^{-5} \text{ rad/s}$ and with altering T_{irr} . The coloured lines indicate momenta profiles along the equator and its coordinates by the colourbar. The dotted black thin line shows momenta profiles at the latitudes 87°N and 87°S . The bold coloured lines represent momenta profiles at the western, eastern terminators, sub- and antistellar point. The grey lines represents all the other momenta profiles.

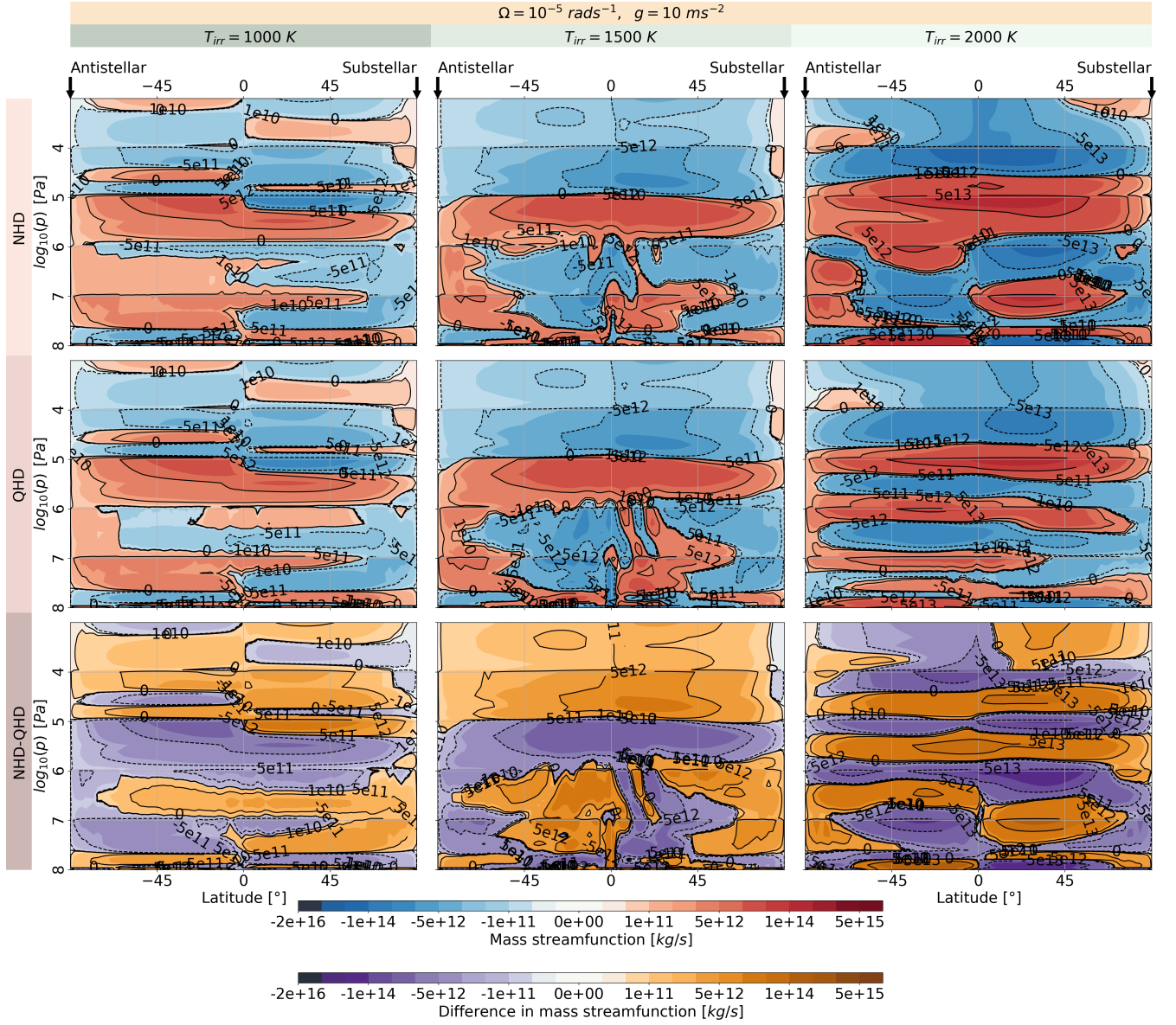


Figure 30. Overturning circulation depicted by the streamfunction Ψ' for the NHD and QHD equation sets with $g = 10 \text{ ms}^{-2}$, $\Omega = 1 \cdot 10^{-5} \text{ rad/s}$ and with altering T_{irr} .

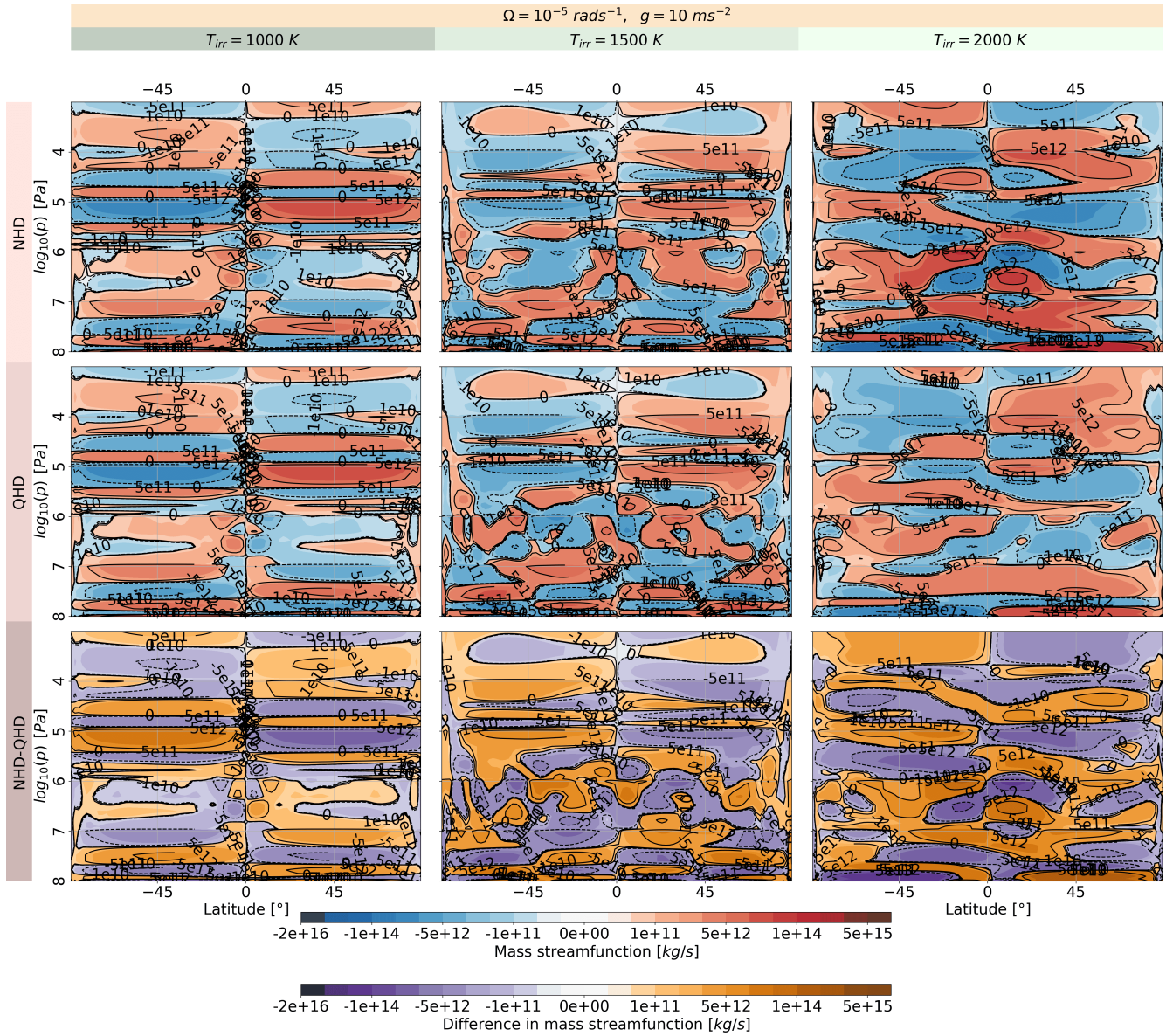


Figure 31. Overturning circulation depicted by the streamfunction Ψ for the NHD and QHD equation sets with $g = 10 \text{ ms}^{-2}$, $\Omega = 1 \cdot 10^{-5} \text{ rad/s}$ and with altering T_{irr} .

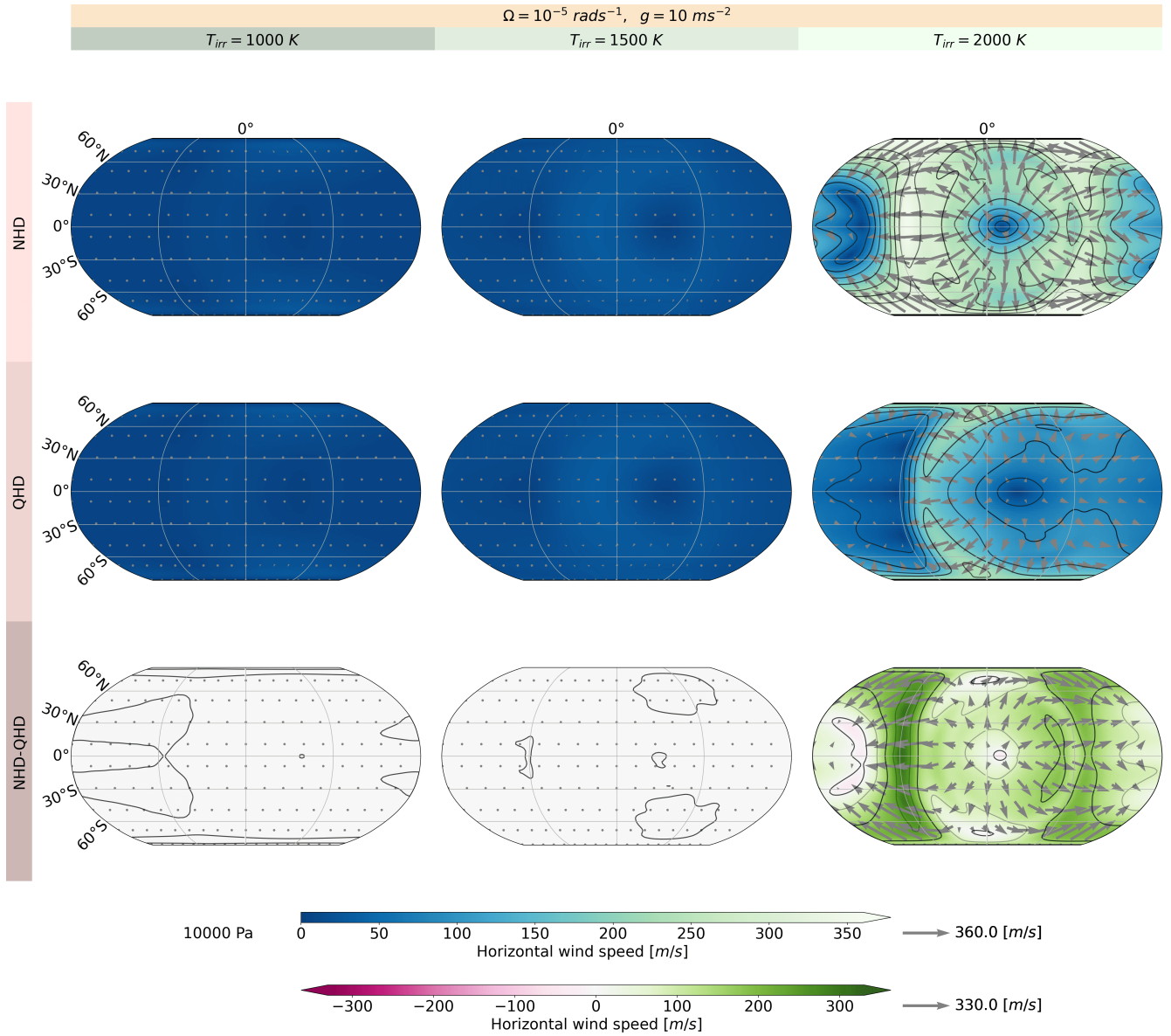


Figure 32. Divergent component of the Helmholtz decomposition for the NHD and QHD equation sets with $g = 10 \text{ ms}^{-2}$, $\Omega = 1 \cdot 10^{-5} \text{ rad/s}$ and with altering T_{irr} .

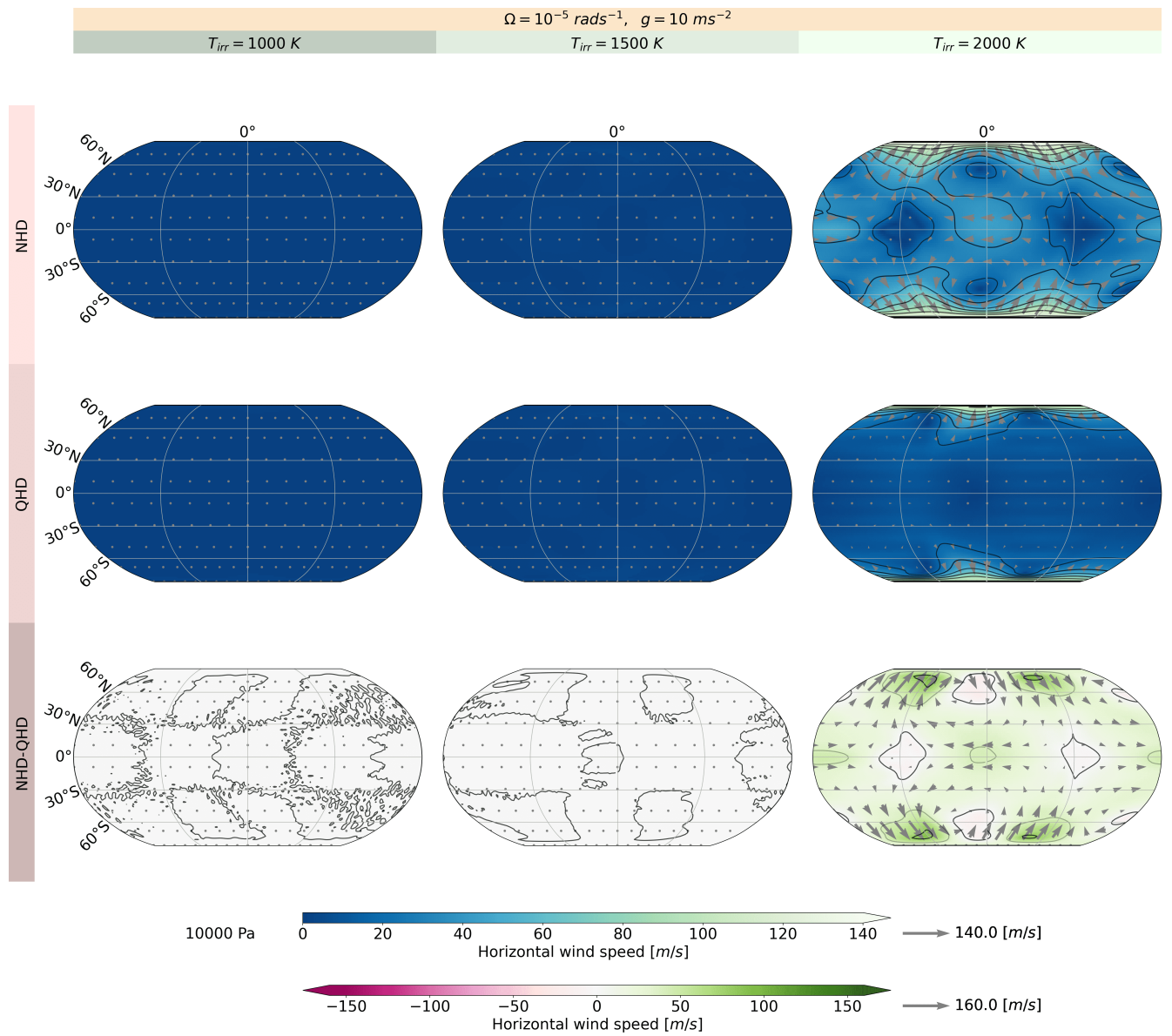


Figure 33. Rotational eddy component of the Helmholtz decomposition for the NHD and QHD equation sets with $g = 10 \text{ ms}^{-2}$, $\Omega = 1 \cdot 10^{-5} \text{ rad/s}$ and with altering T_{irr} .

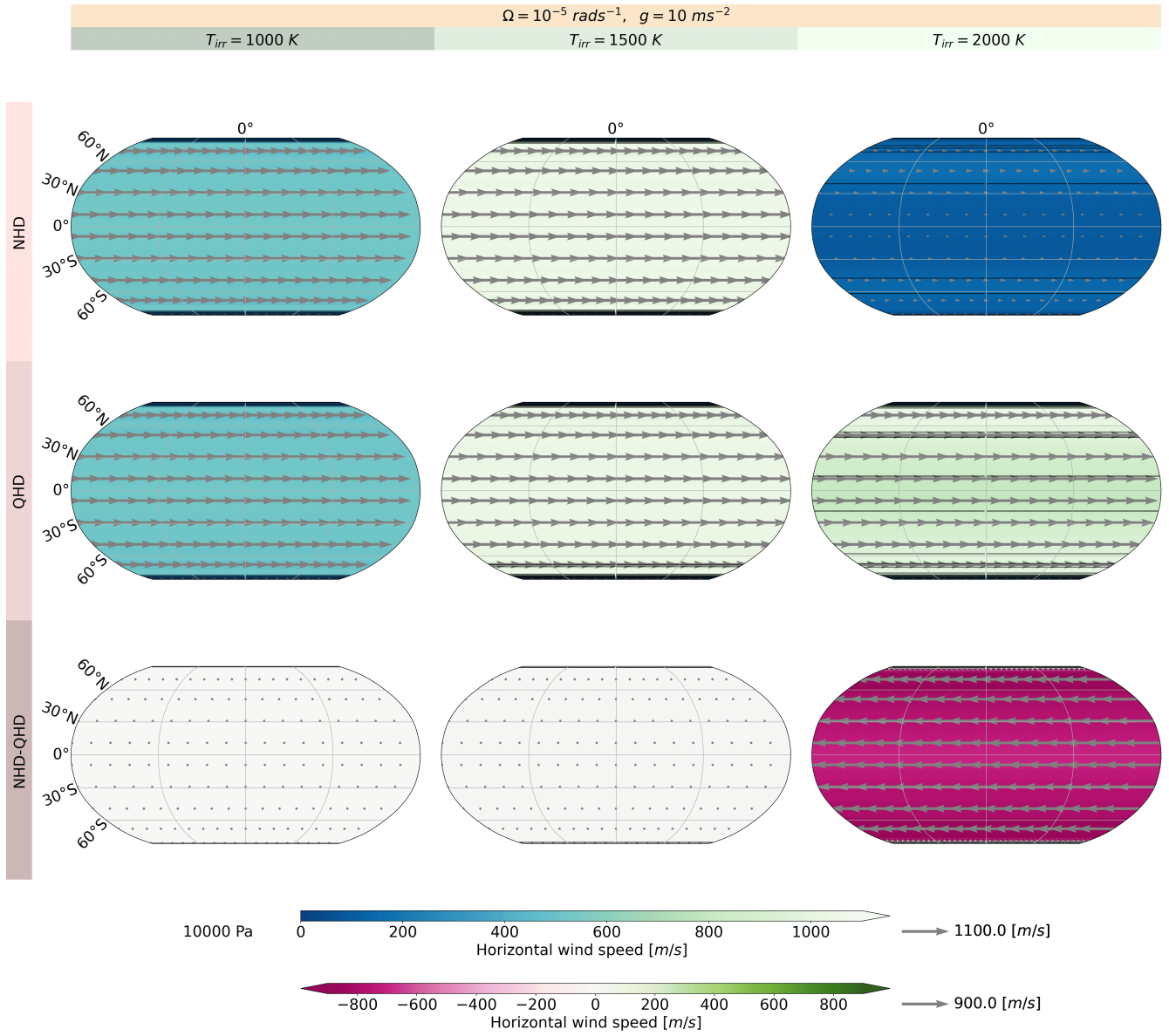


Figure 34. Rotational jet component of the Helmholtz decomposition for the NHD and QHD equation sets with $g = 10 \text{ ms}^{-2}$, $\Omega = 1 \cdot 10^{-5} \text{ rad/s}$ and with altering T_{irr} .

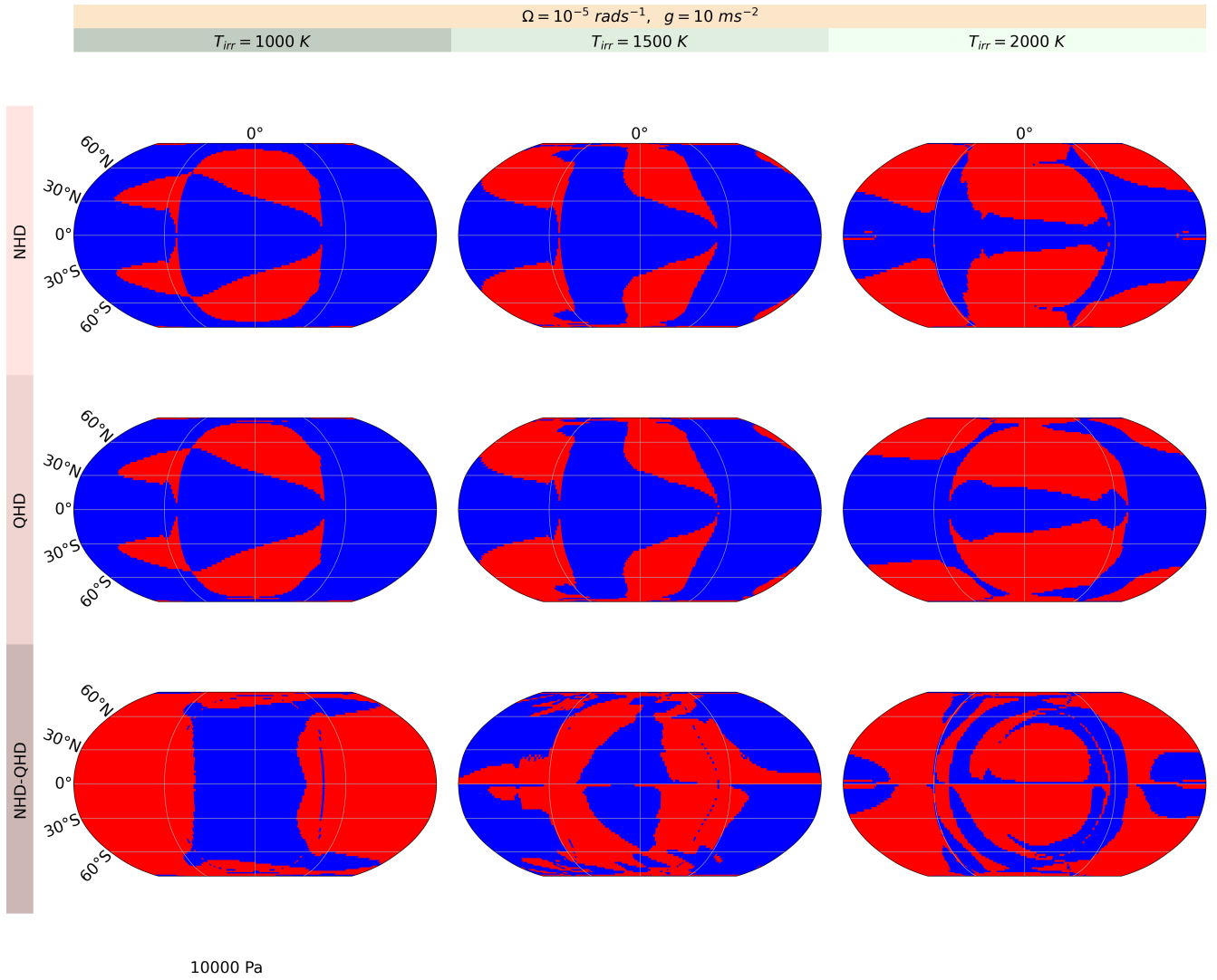


Figure 35. Sign of $\frac{v \tan(\Phi)}{10w} - 1$ for the NHD and QHD equation sets with $g = 10 \text{ ms}^{-2}$, $\Omega = 1 \cdot 10^{-5} \text{ rad/s}$ and with altering T_{irr} . Blue and red regions show negative and positive values

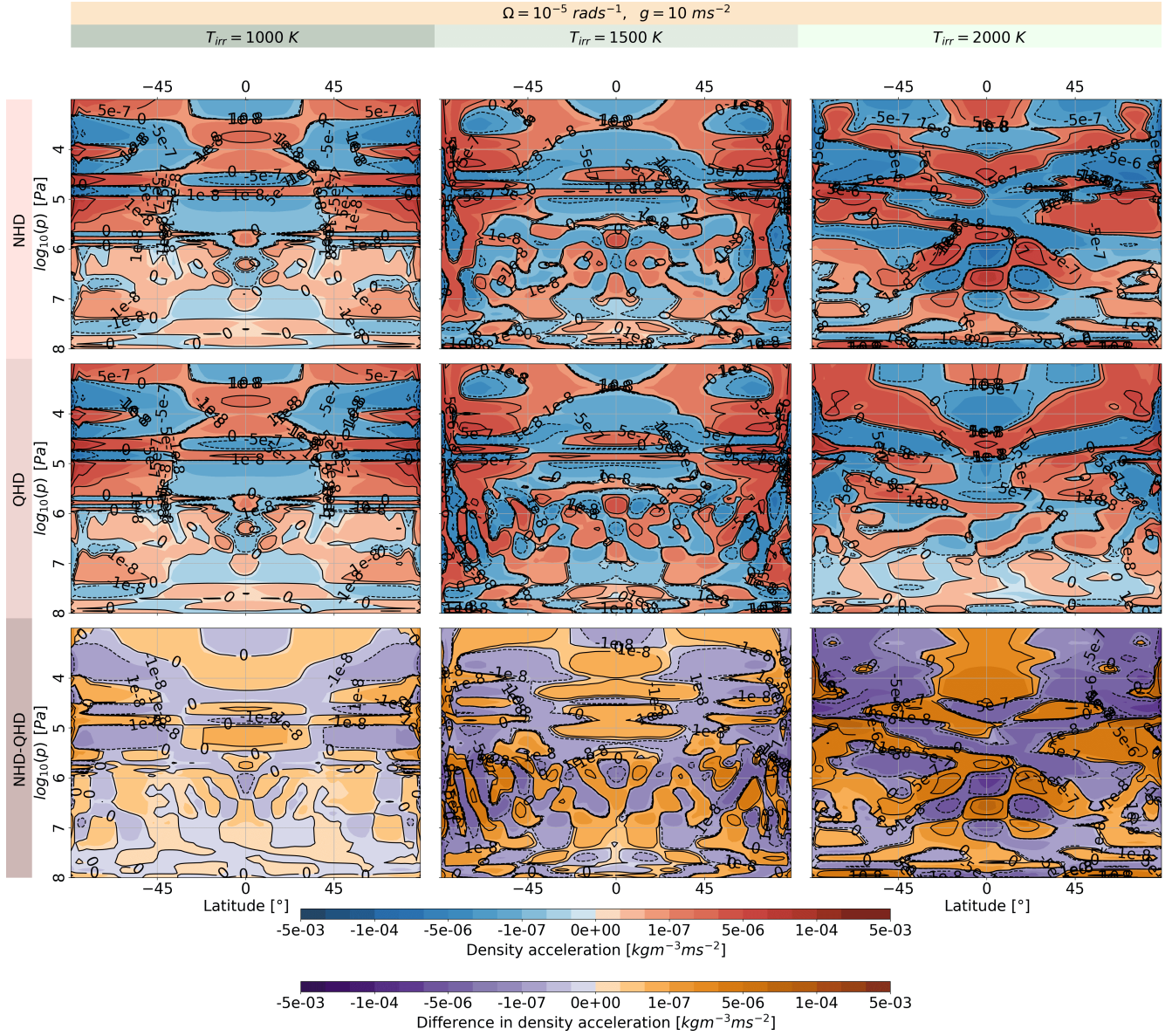


Figure 36. Horizontal acceleration for the NHD and QHD equation sets with $\Omega = 1 \cdot 10^{-5} \text{ rad/s}$, $g = 10 \text{ ms}^{-2}$ and with altering T_{irr} .

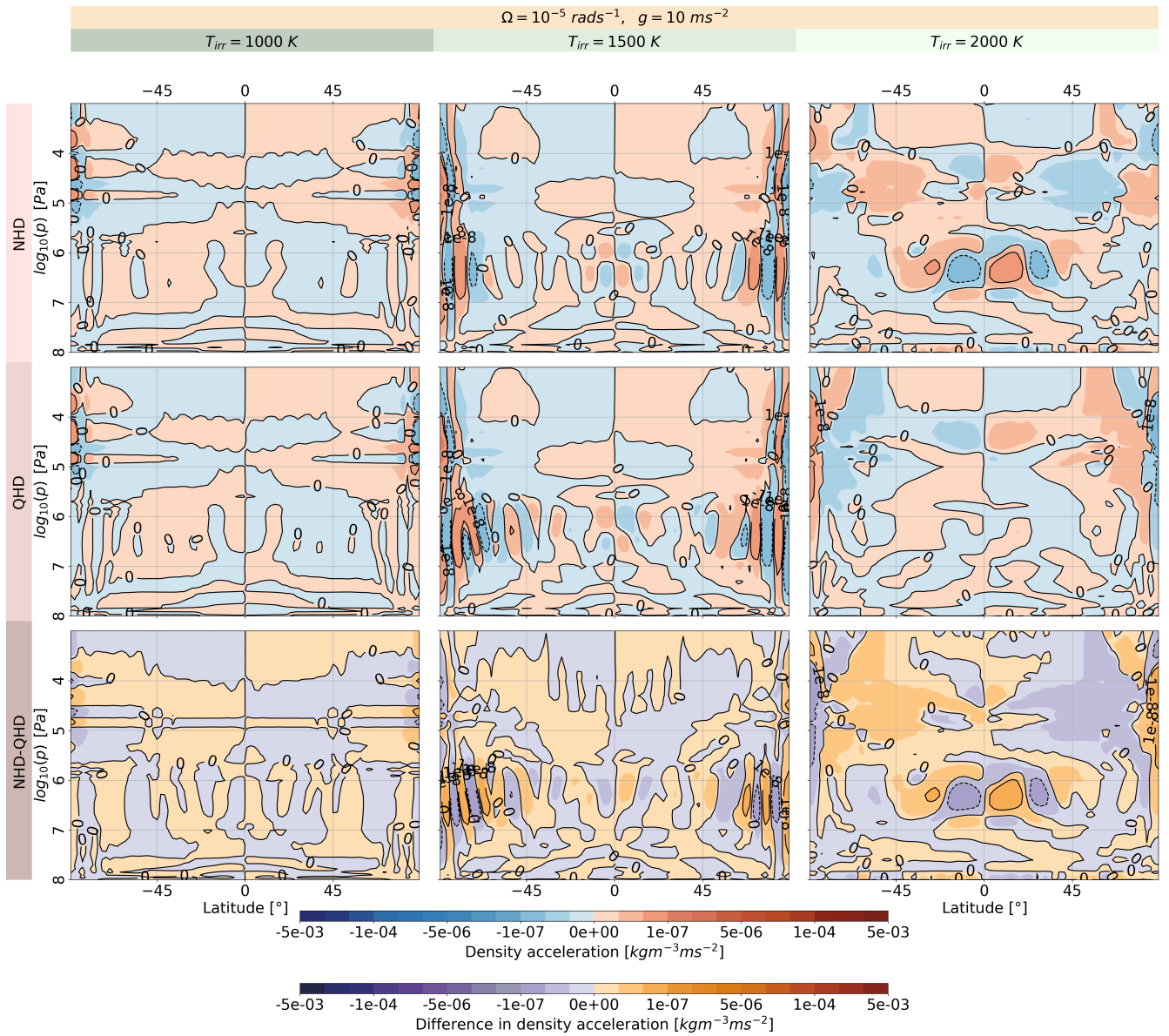


Figure 37. Vertical acceleration for the NHD and QHD equation sets with $\Omega = 1 \cdot 10^{-5} \text{ rad/s}$, $g = 10 \text{ ms}^{-2}$ and with altering T_{irr} .

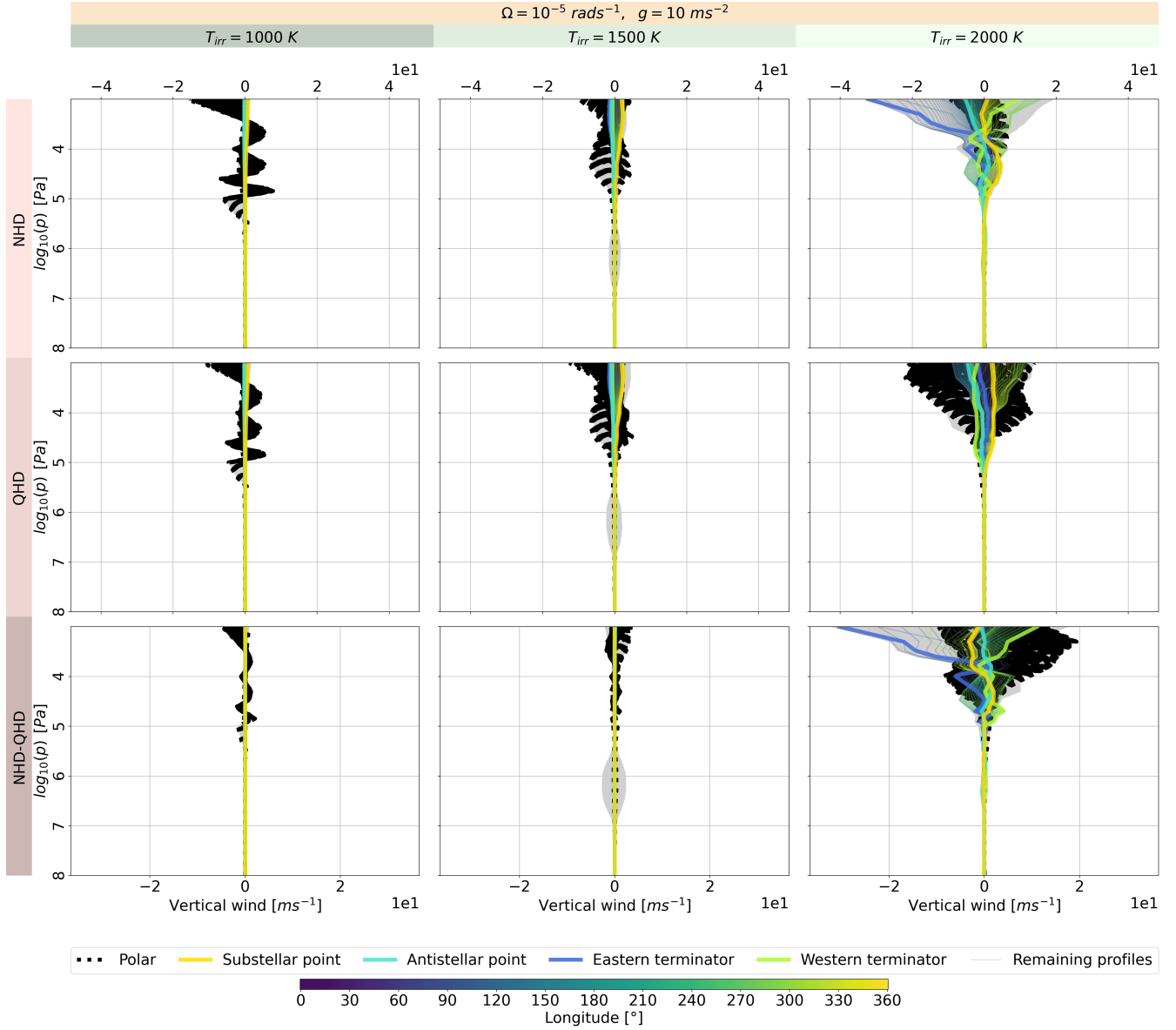


Figure 38. Vertical wind speed at each grid point for the NHD and QHD equation sets with $g = 10 \text{ ms}^{-2}$, $\Omega = 1 \cdot 10^{-5} \text{ rad/s}$ and with altering T_{irr} . The coloured lines indicate momenta profiles along the equator and its coordinates by the colourbar. The dotted black thin line shows momenta profiles at the latitudes 87°N and 87°S . The bold coloured lines represent momenta profiles at the western, eastern terminators, sub- and antistellar point. The grey lines represents all the other momenta profiles.

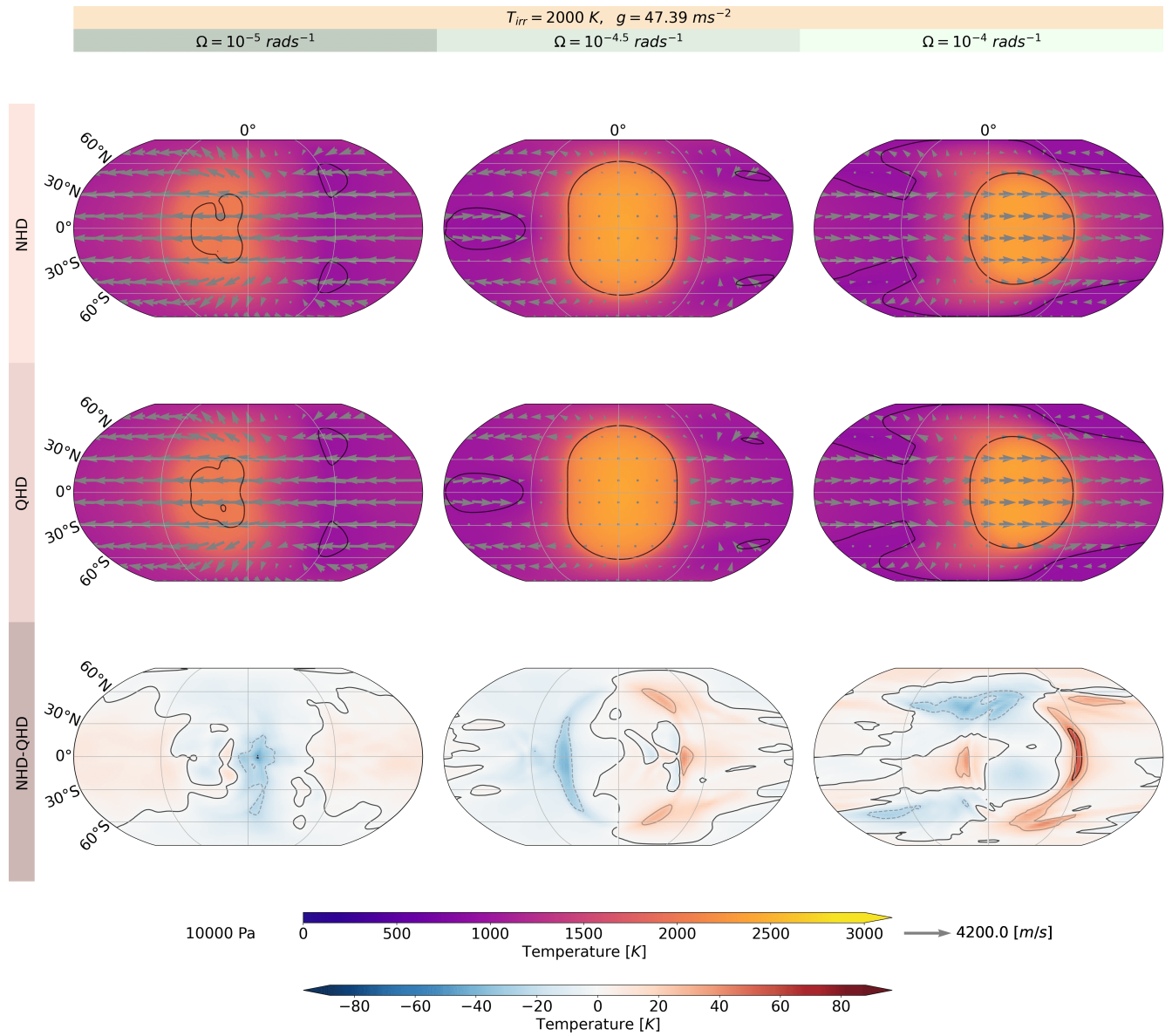


Figure 39. Temperature and wind speed at 10'000 Pa for the the NHD and QHD equation sets with $g = 47.39 \text{ ms}^{-2}$, $T_{irr} = 2'000 \text{ K}$ and with altering Ω .

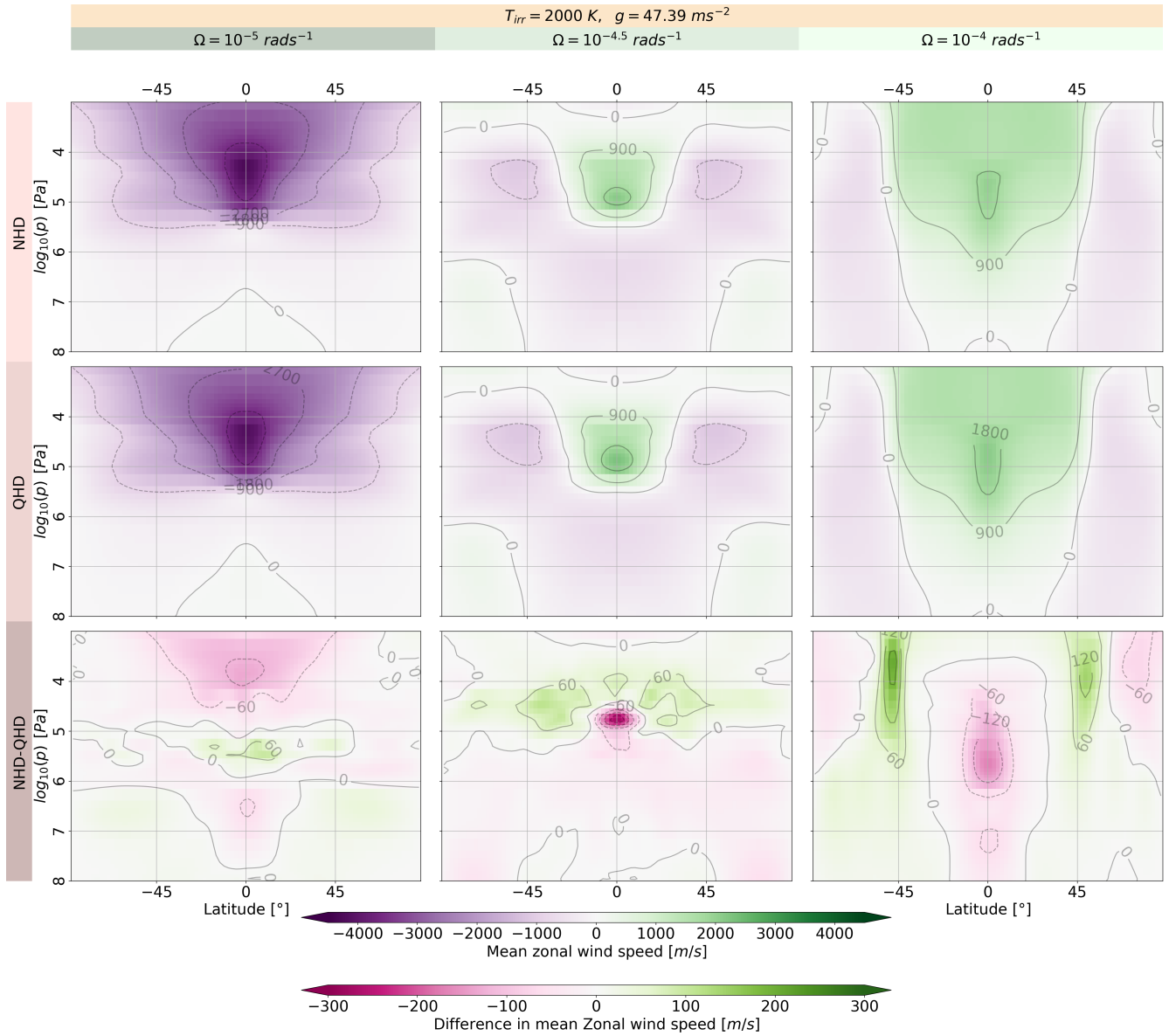


Figure 40. Zonal mean wind at each grid point for the NHD and QHD equation sets with $g = 47.39 \text{ ms}^{-2}$, $T_{irr} = 2'000 \text{ K}$ and with altering Ω .

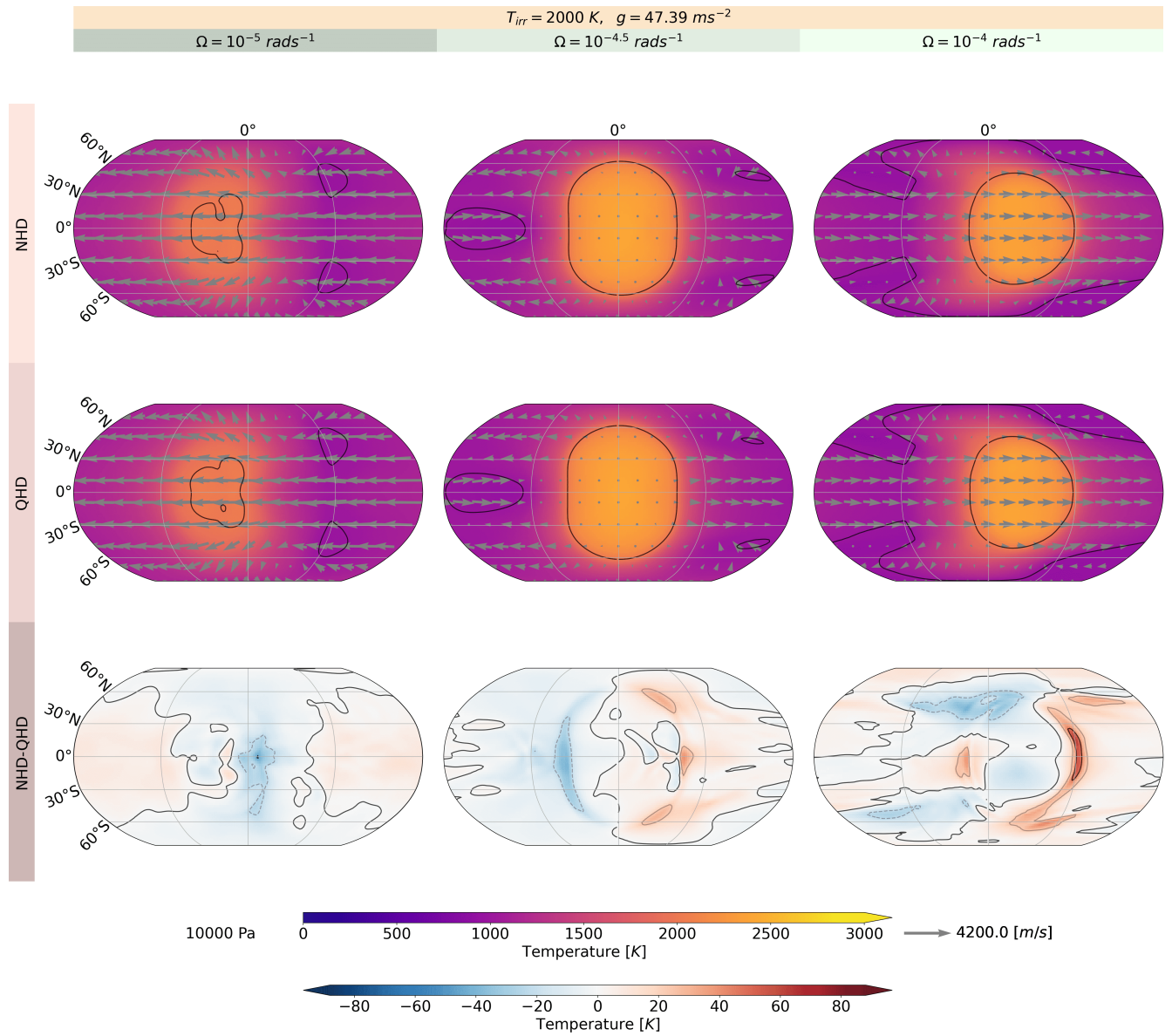


Figure 41. Temperature and wind speed at $10'000 \text{ Pa}$ for the the NHD and QHD equation sets with $g = 47.39 \text{ ms}^{-2}$, $\Omega = 1 \cdot 10^{-5} \text{ rad/s}$ and with altering T_{irr} .

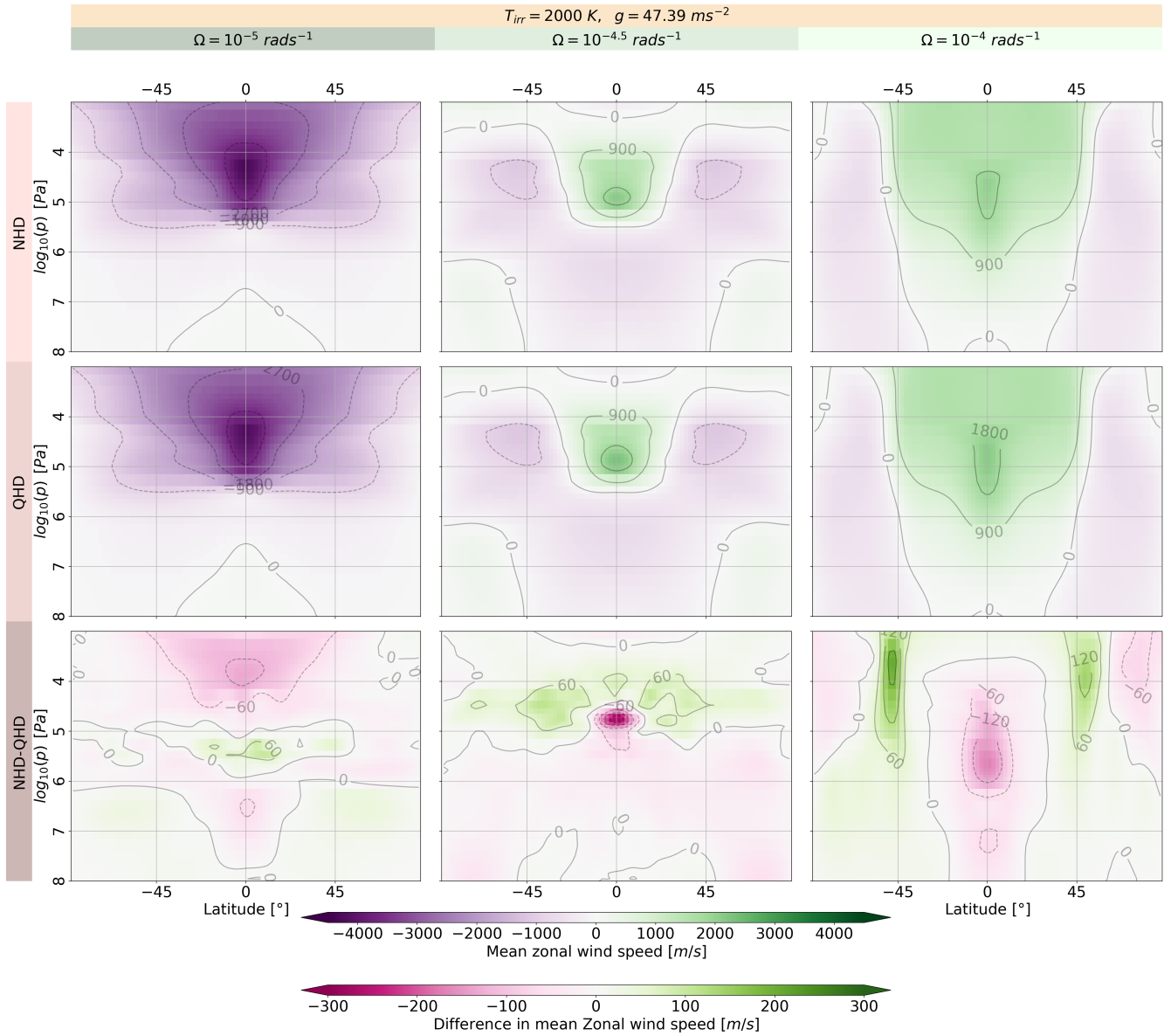


Figure 42. Zonal mean wind at each grid point for the NHD and QHD equation sets with $g = 47.39 \text{ ms}^{-2}$, $\Omega = 1 \cdot 10^{-5} \text{ rad/s}$ and with altering T_{irr} .